

1 **Impacts of climate and land use changes on the hydrological and erosion**
2 **processes of two contrasting Mediterranean catchments**

3

4 **D. Serpa¹, J.P. Nunes^{1,*}, J. Santos¹, E. Sampaio², R. Jacinto¹, S. Veiga², J.C. Lima², M. Moreira², J.**
5 **Corte-Real², J.J. Keizer¹, N. Abrantes¹**

6

7 ¹CESAM & Department of Environment and Planning, University of Aveiro, Campus de Santiago,
8 3810-193 Aveiro, Portugal.

9 ²ICAAM – Institute of Mediterranean Agricultural and Environmental Sciences, University of Évora,
10 Apartado 94, 7006-554 Évora, Portugal.

11

12 *Correspondence to:* jpcn@ua.pt

13

14 **Keywords:** hydrology; erosion; Mediterranean; climate change; land use change

15

16

17

18

19

20

21

22

23

24

25

26

27 **Abstract**

28 The impacts of climate and land use changes on streamflow and sediment export were evaluated
29 for a humid (São Lourenço) and a dry (Guadalupe) Mediterranean catchment, using the SWAT
30 model. SWAT was able to produce viable streamflow and sediment export simulations for both
31 catchments, which provided a baseline for investigating climate and land use changes under the
32 A1B and B1 emission scenarios for 2071-2100. Compared to the baseline scenario (1971-2000),
33 climate change scenarios showed a decrease in annual rainfall for both catchments (humid: -12%;
34 dry: -8%), together with strong increases in rainfall during winter. Land use changes were derived
35 from a socio-economic storyline in which traditional agriculture is replaced by more profitable land
36 uses (i.e. corn and commercial forestry at the humid site; sunflower at the dry site). Climate change
37 projections showed a decrease in streamflow for both catchments, whereas sediments export
38 decreased only for the São Lourenço catchment. Land use changes resulted in an increase in
39 streamflow, but the erosive response differed between catchments. The combination of climate
40 and land use change scenarios led to a reduction in streamflow for both catchments, suggesting a
41 domain of the climatic response. As for sediments, contrasting results were observed for the humid
42 (A1B: -29%; B1: -22%) and dry catchment (A1B: +222%; B1: +5%), which is mainly due to differences
43 in the present-day and forecasted vegetation types. The results highlight the importance of climate-
44 induced land-use change impacts, which could be similar to or more severe than the direct impacts
45 of climate change alone.

46

47

48 **1 Introduction**

49

50 The impact of changes in climate and land cover on watershed dynamics has been well established
51 worldwide. Among the most important impacts from a watershed management perspective are
52 potential alterations to the hydrological (Bangash et al., 2013; Kalantari et al. 2014; Khoi and

53 Suetsugi, 2014; Luo et al., 2013; Mango et al., 2011; Milly et al., 2005; Montenegro and Ragab,
54 2012; Mourato et al., 2015; Wilson and Weng, 2011) and erosive response (Bangash et al., 2013;
55 García-Ruiz et al. 2013; Khoi and Suetsugi, 2014; Lu et al., 2013; Vanmaercke et al., 2011; Wilson
56 and Weng, 2011). These changes will in turn affect the ecosystem service functioning of
57 watersheds, such as water provisioning and erosion control (Bangash et al., 2013).

58 The Mediterranean Basin has been identified as one of the most vulnerable regions of the
59 world to climate change, and the Intergovernmental Panel on Climate Change's Fifth Assessment
60 Report points to projected changes to both the hydrological and erosive response of watersheds
61 due to future shifts in precipitation and temperature regimes (IPCC, 2013). Under the projected
62 climate changes, runoff is expected to decrease (IPCC, 2007, 2013; Nunes et al., 2008) as a result of
63 lower rainfall, higher soil water deficits, and higher potential evapotranspiration (PET) (Molina-
64 Navarro et al., 2014; Nunes et al., 2008, 2013), thereby leading to a decrease in streamflow (López-
65 Moreno et al., 2011, 2014; Molina-Navarro et al., 2014). As for soil erosion, there is greater
66 heterogeneity in the trends across the Mediterranean Basin, as the processes linking climate and
67 erosion are dependent on a number of variables; including rainfall amount and intensity, soil water
68 content, evapotranspiration, and plant cover (García-Ruiz et al. 2013; Nearing et al., 2005; Nunes
69 and Nearing, 2011).

70 The magnitude of climate change impacts on hydrological and erosion processes is expected
71 to be strongly influenced by land use/cover, as this driver *per se* is known to strongly influence these
72 processes (Cerdan et al. 2010; García-Ruiz and Lana-Renault, 2011; García-Ruiz et al. 2013; Nunes
73 and Nearing, 2011). Several studies conducted in the Mediterranean Basin have indicated that the
74 hydrological behaviour of different land-cover types is linked to the existing vegetation and to its
75 spatial and seasonal variation patterns (García-Ruiz and Lana-Renault, 2011; López-Vicente et al.,
76 2013; Nunes et al., 2010, 2011). For example, a rise in shrub and forest cover has been reported to
77 produce a decline in surface runoff and streamflow discharge (Begueria et al., 2003; Gallart and
78 Llorens, 2004; García-Ruiz and Lana-Renault, 2011). Land cover also affects soil erosion, as land with

79 permanent vegetation cover (shrub, grassland, or forest) typically has lower soil losses and
80 sediment yields than an arable land (Cerdan et al. 2010; García-Ruiz, 2010).

81 While it is important to consider the individual effects of climate and land use change on
82 hydrological and erosion processes, assessing how their combined effects will interact is crucial for
83 assessments of the future state of water resources (Hoque et al., 2014; Khoi and Suetsugi, 2014; Li
84 et al., 2004; Li et al., 2009; Li et al. 2012). For the Mediterranean region, only a few modelling studies
85 have addressed the combined effects of these drivers (e.g. López-Moreno et al., 2014; Molina-
86 Navarro et al., 2014). Most studies have focused on the effects of climate change without
87 considering land use/cover change as well (Nunes et al., 2008, 2013; Bangash et al., 2013;
88 Kalogeropoulos and Chalkias, 2013; Zabaleta et al., 2014). Others have only evaluated the impacts
89 of land use changes without considering future climate conditions (De Girolamo and Lo Porto, 2012;
90 López-Vicente et al., 2013; Nunes et al., 2011).

91 All climate and land use change assessment studies have associated uncertainties in the model
92 results and the selected scenarios (see e.g. Ludwig et al., 2010, for a discussion on this issue).
93 Uncertainties in observed data can mislead model calibration (McMillan et al., 2010; Sellami et al.,
94 2013), and the existence of multiple acceptable model formulations and/or parameterizations can
95 lead to different results for different climate conditions (Beven, 2012; Lespinas et al., 2014).
96 Calibrated model parameters often compensate for shortcomings in the model structure and errors
97 in data (Lespinas et al., 2014). Therefore, uncertainty issues can be partly overcome by restricting
98 possible parameter values through direct measurement, by using multiple observed variables in the
99 calibration process (Beven, 2012; Efstratiadis and Koutsoyiannis, 2010), and by evaluating the
100 model for a large range of climatic conditions (Beven, 2012; Xu and Singh, 2004).

101 Scenario uncertainties include different projections of socio-economic conditions and
102 greenhouse gas emission (IPCC, 2007, 2013); different response of climate to greenhouse gas
103 concentrations given by different Global Circulation Models (GCMs); different climate downscaling
104 results according to the selection of Regional Climate Models (RCMs) or statistical approaches

105 (Deidda et al., 2013; Maraun et al., 2010); or different land-use scenarios according to different
106 interpretations of future socio-economic conditions (e.g. Stigter et al., 2015). The variability
107 between these scenarios for the Mediterranean can lead to quite different projections of
108 hydrological change (Majone et al., 2015; Piras et al., 2014; Stigter et al., 2014). To mitigate this
109 issue, a smaller number of future scenarios (or even hypothetical scenarios) can be analyzed to
110 detail particular impacts, becoming in effect a study of sensitivity to climate and land use change
111 (Nunes et al., 2008, 2013; Xu and Singh, 2004).

112 In this work, the impacts of climate and land use changes on streamflow discharge and
113 sediment export were evaluated both individually, to assess the relative strength of their impacts;
114 and in an integrated manner, to provide a more realistic assessment of future (combined) impacts.
115 This study was performed in two small experimental Portuguese basins (i.e. a paired-catchment
116 approach), one located in a humid region (São Lourenço) and the other in a dry region (Guadalupe).
117 These catchments were selected because: (i) each catchment is representative of the landscapes in
118 their region (i.e. north-western and interior-southern Portugal); (ii) the responses to climate and
119 land use changes are expected to differ in each of these regions due to their contrasting climate,
120 soil, and land cover characteristics; and (iii) the availability of several measured parameters and
121 hydrological variables reduces model uncertainty. A limited number of climate and land use
122 scenarios were selected to evaluate the sensitivity of the study sites to these changes.

123 The specific objectives of the present study were:

124 i) to calibrate and validate the Soil Water Assessment Tool model (SWAT) for the São Lourenço
125 and Guadalupe basins;

126 ii) to simulate the separate responses of stream discharge and sediment export for two
127 scenarios of climate and land use change;

128 iii) to evaluate the effects of two scenarios combining changes in climate and land use.

129

130 **2 Methodology**

131

132 **2.1 Study sites**

133 The present work was carried out in two small agro-forested catchments in Portugal. The humid
134 catchment – São Lourenço (6.20 km²; Coordinates: 40° 25' 58"N; 8° 30' 6"W) is located in North
135 Central Portugal (Fig. 1), whereas the dry catchment – Guadalupe (4.49 km²; Coordinates: 38° 34'
136 39"N; 8° 2' 26"W) – is located in South Eastern Portugal (Fig. 1).

137 Due to its proximity to the sea, São Lourenço is significantly influenced by the Atlantic Ocean,
138 resulting in mild and wet winters with strong precipitation events and warm and dry summers. The
139 average annual rainfall and temperature in the region (1973 - 2012) was 925 mm and 15.7 °C
140 (SNIRH, 2014a). Elevations range from 40 m a.s.l. to 100 m a.s.l and gentle slopes (<5%) dominate
141 the area (Fig. 2). The soils are dominated by Humic Cambisols (50%) with high depth and high
142 organic matter content; with a significant proportion of Chromic Luvisols (23%) and Calcaric
143 Cambisols (18%) in the watershed (Fig. 2; DGADR, 2013). As part of an important Portuguese
144 winegrowing region – the Bairrada – almost half of the São Lourenço basin is occupied by vineyards
145 whereas the remaining area is mostly maritime pine plantations and annual rain-fed crops, such as
146 corn, potato, and pasture (Fig 2).

147 In contrast, Guadalupe has typical inland Mediterranean climate, characterized by highly
148 variable rainfall, few flood events, and an ephemeral watercourse. The average annual rainfall and
149 temperature (1973 - 2012) in Guadalupe was considerably drier (533 mm) than São Lourenço, but
150 differed little in temperature (15.5 °C) (SNIRH, 2014a). The watershed is dominated by moderate
151 slopes (10%) (Fig. 3), and is located between 260 to 380 m a.s.l.. The predominant soils are relatively
152 shallow Cambisols (54%), Luvisols (22%), and Leptosols (21%), which are associated with the intense
153 agricultural production of the watershed in the last decades. This land use has led to severe
154 problems of land degradation, and the area has been identified as having a high risk of
155 desertification (Nunes et al., 2008). As in other dry regions of southern Portugal and Spain,

156 Guadalupe is dominated by the “montado” agro-forestry system, where open cork oak stands are
157 interspersed with annual crops and pastures (Fig. 3).

158

159 **2.2 Hydrological modelling**

160 The SWAT model (Neitsch et al., 2011) has been widely applied to different size watersheds and
161 applications all over the world, including assessments of the effects of climate and land-cover
162 change on water quantity and soil erosion (SWAT Database, 2014).

163 SWAT is a conceptual, time-continuous and semi-distributed hydrologic model initially
164 developed to predict changes in landscape management practices on water, sediment, and
165 chemical yields (Arnold et al., 1998; Neitsch et al., 2011). However, its structure also allows SWAT
166 to explicitly account for climate and land use changes. For instance, the model is able to simulate
167 the impacts of temperature changes and soil water deficit on vegetation growth, as well as the
168 effects of climate change on the water balance, and therefore on the processes controlling surface
169 and base flow generation (Neitsch et al., 2011). By simulating changes in vegetation and runoff,
170 SWAT is also able to predict the erosive response. Regarding the effects of land use changes, the
171 model allow for simulation of alternative land use distributions, which in turn affects all the other
172 processes, i.e. water balance, runoff generation, and soil erosion (Neitsch et al., 2011).

173 SWAT typically operates on a daily time step and accounts for spatial heterogeneities by
174 dividing the watershed into sub-basins, which are further divided into one or more Hydrologic
175 Response Units (HRUs). Each HRU consists of a unique combination of soil, slope, and land use.

176 The hydrological component of SWAT calculates the daily water balance for each HRU. The
177 model takes into account precipitation, evapotranspiration, soil water balance, surface runoff,
178 subsurface runoff, and aquifer recharge. From the available methods for calculating
179 evapotranspiration in SWAT, the Hargreaves method (Hargreaves et al., 1985) was selected for the
180 present study. Regarding runoff, the model uses the Soil Conservation Service Curve Number
181 method (SCS, 1985) to estimate surface runoff and a kinematic percolation model to predict

182 subsurface runoff (Neitsch et al., 2002). Predictions of peak runoff rates for each HRU are made
183 using the rational method (Neitsch et al., 2002). Once the model determines the water loadings
184 from each HRU, the water flow is routed through the main channel using the variable storage
185 coefficient method (Neitsch et al., 2011).

186 In SWAT, soil erosion is calculated according to the Modified Universal Soil Loss Equation –
187 MUSLE (Neitsch et al., 2011). Sediment loadings from each HRU are then summed at the sub-basin
188 level, and the resulting loads are routed by streamflow and distributed to the watershed outlet.
189 Sediment transport in the channel network is controlled simultaneously by deposition and
190 degradation processes, which depend on the sediment loads coming from upland areas and on the
191 channel transport capacity.

192 A complete description of the SWAT model and theory can be found in Neitsch et al. (2011)
193 and Arnold et al. (2011).

194

195 **2.2.1 Model set-up and input data**

196 SWAT requires as input hydro-meteorological data, a land-cover map, a soil map, and a Digital
197 Elevation Model (DEM); the source of which for the present study is summarized in Table 1. After
198 data compilation, ArcSWAT version 9.3 (Neitsch et al., 2011) was used for watershed delineation
199 and sub-basin discretization using the DEM. In both watersheds, 10 sub-basins were delimited and
200 then divided into multiple HRUs (123 in São Lourenço and 107 in Guadalupe) according to the land
201 cover, soil types, and slope classes presented in Figs. 2 and 3.

202 Prior to running the model, SWAT databases (Soils, Land Cover/Plant Growth, Fertilizers,
203 Urban) were modified to account for the specific characteristics of each watershed. Soil
204 parameterization was performed according to the existing literature on Portuguese soils (Cardoso,
205 1965, 1973) and the data collected on soil properties (i.e. soil depth, soil texture, organic matter
206 content, bulk density, hydraulic conductivity) in several soil surveys carried out at the two
207 catchments. As for land cover, parameterization was done according to the literature for

208 Mediterranean vegetation and crops (Nunes et al., 2008). Information on agricultural and
209 fertilization practices as well as other management operations was obtained from the data
210 published by the Portuguese Ministry of Agriculture (INIA-LQARS, 2000).

211

212 **2.2.2 Model calibration, validation and performance evaluation**

213 SWAT was calibrated and validated against streamflow and sediment data collected at the São
214 Lourenço and Guadalupe hydrometric stations, which were installed on April 2012 and April 2011,
215 respectively. Daily streamflow was calculated based on water levels recorded at a 2 minute
216 frequency, and the stage-discharge curve of each basin, which in São Lourenço was measured in an
217 artificial regular channel. Daily sediment data for São Lourenço was obtained by interpolating the
218 measured values of total suspended solids (TSS) in water samples collected by an ISCO3700
219 automatic sampler triggered by a water level sensor through a CR200 data-logger (Campbell
220 Scientific®). The sediment data for Guadalupe was estimated using an OBS-3 optical turbidity sensor
221 (continuous measurements) linked to a CR800 data-logger (Campbell Scientific®), which was
222 calibrated using TSS data from stream water samples collected at various intervals. For São
223 Lourenço, 1-year of data was used for model calibration (May 2012 – May 2013) and another for
224 model validation (May 2013 – May 2014). For Guadalupe, the two periods differed in duration; ca.
225 1.5 years for calibration (September 2011 – May 2013) and 1 year for validation (May 2013 – May
226 2014). Prior to calibration, both models were warmed-up (São Lourenço – 15 years; Guadalupe – 9
227 years) to eliminate initial bias, taking advantage of existing meteorological data.

228 In addition to the streamflow and sediment records, measurements of runoff, erosion and soil
229 moisture were also calibrated. These were conducted at 6 experimental plots implemented in the
230 vineyard and montado area of the São Lourenço and Guadalupe catchments, respectively. For
231 Guadalupe, actual evapotranspiration, leaf area index, and biomass of pasture and montado were
232 also calibrated using data from 2 eddy covariance towers (Gilmanov et al., 2007; Paço et al., 2009;
233 Reichstein et al., 2003). Model calibration was performed manually and on a daily time step;

234 streamflow was first calibrated independently, and then was slightly adjusted during a subsequent
235 calibration of sediment yield. The calibrated model parameters are presented in Table 2.

236 Model performance, defined as the goodness of fit between observed and predicted
237 streamflow and sediment export, was evaluated using the Nash-Sutcliffe coefficient (NSE), and the
238 ratio between the Root Mean Square Error and the sample standard deviation (RSR) (Moriasi et al.,
239 2007). The magnitude of model errors compared to observations was evaluated by the percent of
240 bias, PBIAS (Moriasi et al., 2007). Positive PBIAS values indicate model underestimation, whereas
241 negative values indicate overestimation. According to Moriasi et al. (2007), NSE values greater than
242 0.5 and RSR values below 0.7 indicate reasonable model performance for monthly simulations of
243 streamflow and sediment export. PBIAS values below 25% for streamflow and below 55% for
244 sediments are also considered reasonable (Moriasi et al., 2007).

245

246 **2.3 Climate change scenarios**

247 Climate change scenarios were developed for the period between 2071 and 2100, using the
248 ECHAM5 GCM (Roeckner et al., 2003) driven by the A1B (more severe) and B1 (more moderate)
249 emission scenarios, defined by Nakićenović and Swart (2000). GCM simulations were then
250 statistically downscaled to obtain local daily predictions of rainfall and temperature (Fig. 4), using
251 the predictor transformation approach (Maraun et al., 2010). This methodology is described in
252 detail by Veiga (2013), and uses Mean Sea Level Pressure (MSLP) in the Atlantic Ocean as a predictor
253 since it is related with climate in Portugal (e.g. Corte-Real et al., 1998). The methodology consists
254 of three consecutive steps:

255 1) A relationship was established between the historical MSLP in the Atlantic Ocean (Compo et
256 al., 2011) and rainfall and temperature at two meteorological stations: Coimbra (close to S.
257 Lourenço) and Évora (close to Guadalupe). The relationship with rainfall was determined for 1950-
258 2000 at the seasonal scale using canonical correlation analysis, while the relationship with

259 temperature was determined for 1970-2000 at the monthly scale using stepwise multiple linear
260 regressions.

261 2) Future MSLP was estimated from anomalies between ECHAM5 predictions for 2071-2100 and
262 1971-2000 (reference period) for both the A1B and B1 scenarios. The resulting MSLP predictions
263 were used to calculate a first estimate of future seasonal rainfall and monthly temperature using
264 the above-mentioned relationship. The final estimate of seasonal rainfall and monthly temperature
265 was calculated from anomalies between MSLP-based estimates for 2071-2100 and 1971-2000 for
266 A1B and B1.

267 3) Daily rainfall and temperature were calculated using the fragments method (Svanidze, 1977).
268 Each future prediction of seasonal rainfall and monthly temperature was compared with the closest
269 period in the historical observations, and the daily values of the historical periods were used to
270 represent the daily values of the future periods.

271 Since this method did not predict noticeable changes to temperature, the resulting daily time-
272 series was further adjusted by adding a fixed anomaly to each day (following Kilsby et al., 2007),
273 which were selected conservatively as the lower bound of forecasts for each study site by the
274 Regional Climate Models used in projects PRUDENCE (Déqué et al., 2005) and ENSEMBLES (Van Der
275 Linden and Mitchell, 2009). The added anomaly was 2.2°C for the A1B scenario and 1.1°C for the B1
276 scenario.

277

278 **2.4 Land use change scenarios**

279 Land use scenarios for both catchments were defined according to the methodology applied by
280 Jacinto et al. (2013), which is shown in Fig. 4. The first step consisted in a linear downscaling of
281 European trends for generic land use types in Portugal (IPCC, 2007; Rounsevell et al., 2006; Verburg
282 et al., 2006). These scenarios forecast a decrease of agricultural area in Portugal for 2100, of 73%
283 and 54% for emissions scenario A1B and B1 respectively, and suggest a number of possible land-
284 cover type replacements including forestry and crops for bio-fuel production.

285 Local trends were then defined based on an analysis of historical land use patterns in order to
286 capture the socio-ecological characteristics of both study sites (Graffin et. al, 2004). This included
287 an analysis of literature of agriculture and forest change (e.g. Jones et al., 2011; Moreira et al., 2001;
288 Tavares et al., 2012), and a comparison of land use between 1990, 2000, and 2006 using Corine
289 land cover maps. These trends were used to identify patterns of land use change in the second half
290 of the 20th century (a period of large-scale agricultural abandonment and afforestation in Portugal)
291 to provide further insights on which types of agricultural areas would preferentially be abandoned
292 at each study site, and what the likely replacing land uses would be.

293 Finally, the socio-economic trends used to generate scenarios A1B and B1 were analyzed to gain
294 insight into the driving forces behind land use changes, taking into account that the A1B scenario
295 would put greater emphasis on economic value while the B1 scenario would also emphasize nature
296 conservation values (IPCC, 2007). Generic land use change rules for A1B and B1 were created from
297 IPCC (2007), Rounsevell et al. (2006) and Verburg et al. (2006). These generic rules were combined
298 with the local trend analysis to define: (i) the most likely crops subject to abandonment in the A1B
299 and B1 scenarios, assuming a similar degree of abandonment as forecasted at the Portuguese scale;
300 and (ii) likely replacement land-cover or crops in the A1B and B1 scenarios. This approach ensured
301 consistency between climate and land use changes since land use scenarios followed the same
302 storylines as climate change scenarios.

303

304 **3 Results**

305

306 **3.1 Model calibration and validation**

307 The model results based on the performance indicators considered in the present study are shown
308 in Table 3. A good agreement was found between observed and predicted monthly streamflow for
309 both catchments and for both the calibration and validation period. The sediment export predicted
310 for São Lourenço fit reasonably well with the measured values, despite some model

311 underestimation in both the calibration (PBIAS = 28%) and validation period (PBIAS = 32%). For the
312 sediment export in the Guadalupe catchment, model performance might be considered reasonable
313 for the validation period but not for the calibration period (Table 3).

314 Model performance for daily streamflow and sediment export (Figs. 5 and 6) was worse than
315 for monthly values, particularly in Guadalupe (Table 3).

316

317 **3.2 Future scenarios**

318 **3.2.1 Climate change scenarios**

319 Compared to the baseline period of 1971 to 2000, the forecasts for 2071 to 2100 indicated a small
320 decrease in annual rainfall for both São Lourenço (ca. 12%) and Guadalupe (ca. 8%) together with
321 higher rainfall in winter, on average 19% and 40% respectively, for the humid and dry catchment
322 (Fig. 7). For both catchments, the A1B and B1 scenarios differed mainly in seasonal rainfall
323 distribution, but not in the annual rainfall volumes (Fig. 7). Due to the downscaling method used
324 (see Section 2.3), the same changes in average annual temperature were predicted for the two
325 catchments (Fig. 7): an increase of 2.2°C was forecasted for scenario A1B as opposed to an increase
326 of 1.1°C for scenario B1.

327

328 **3.2.2 Land use change scenarios**

329 Future land use changes for the São Lourenço and Guadalupe catchments are presented in Tables
330 4 and 5, respectively. In accordance with the forecasts for Portugal as described earlier, a large
331 decrease in agricultural lands for food production was assumed under scenarios A1B and B1, but
332 with a larger change in the A1B scenario.

333 The differences between the study sites are related to the different historical land use change
334 trends in the latter half of the 20th century, as described above. In the northern region, traditional
335 agricultural crops such as potato and pastures were predicted to be replaced primarily by corn (for
336 biofuel production) and by commercial forests (Table 4), all of which are already present locally. In

337 the southern region, traditional crops (wheat and other cereals) and pasture are predicted to be
338 replaced by sunflower for biofuel production and abandoned to become shrublands (Table 5).
339 While sunflower is not present locally, it is cultivated in other places in southern Portugal and has
340 a high potential to tolerate the warmer and drier conditions forecasted under climate change
341 (Camacho-B et al., 1974).

342 The differences between the A1B and B1 scenarios are related to their storylines, also as
343 described above. Hence the A1B scenario is more focused on economic development, whereas the
344 B1 scenario is more directed towards environmentally-friendly options (IPCC, 2007). Under scenario
345 A1B, the existing permanent pastures and mixed forests in São Lourenço were foreseen to be
346 converted into eucalypt forests, because this is a more valuable species from the economic point
347 of view. Under the B1 scenario these areas were converted into pine forests, as it is a more
348 appropriate species from an environmental point of view (Table 4). Likewise, small vineyard areas
349 in São Lourenço were assumed to be replaced by corn and eucalypt plantations under the A1B
350 scenario and to be maintained under scenario B1.

351 For Guadalupe, the areas permanently occupied by pastures were assumed to be converted
352 into sunflower plantations to a much larger extent under the A1B scenario than under the B1
353 scenario (Table 5). As for pastures associated with the “montado” system, in areas where oak cover
354 is currently less than 50%, pastures were assumed to be fully converted into sunflower plantations
355 under the A1B scenario, but maintained under the B1 scenario. In areas with more than 50% oak
356 cover, pastures were assumed to be abandoned and naturally replaced by Mediterranean
357 shrublands for both scenarios.

358

359 **3.3 Effects of climate changes**

360 Under both climate change scenarios, annual streamflow was forecasted to decrease by 13% in the
361 São Lourenço basin (Fig. 8). This decrease in streamflow was accompanied by large decreases in
362 actual evapotranspiration (ET) by the main land cover types of vine (-10 to -11%) and maritime pine

363 (-7 to -8%), as shown in Table 6. In Guadalupe, the reduction in streamflow was higher (Fig. 8), from
364 a 14% reduction in the A1B scenario, to an 18% decrease in the B1 scenario. However, the decreases
365 in actual ET from the main land cover types of oak (-4 to -6%) and pasture (-4 to -5%) were smaller
366 than in the humid catchment (Table 7).

367 Regarding sediment export, the model predicted a decrease of 9% in the A1B scenario and of
368 11% in the B1 scenario for the São Lourenço basin (Fig. 9). For Guadalupe, an increase in sediment
369 export of 24% and 22% was forecasted for the A1B and the B1 scenarios respectively (Fig. 9).

370

371 **3.4 Effects of land use changes**

372 In contrast to the predicted climate change impacts, land use changes led to a small increase in
373 average annual streamflow for both catchments (São Lourenço: 0.2 – 1%; Guadalupe: 0.3 – 6%)
374 under both scenario A1B and B1 (Fig. 8).

375 Sediment export exhibited different behaviors in the two catchments. In São Lourenço, a
376 decrease of 10% (B1 scenario) and 18% (A1B scenario) in annual sediment export was predicted
377 due to land use changes (Fig. 9). In Guadalupe, erosion was forecasted to increase for both
378 scenarios, by 257% in the A1B scenario and by 9% in the B1 scenario.

379

380 **3.5 Combined effects of climate and land use changes**

381 For both basins, the decrease in streamflow caused by climate change was offset by the increase
382 caused by land use changes (Figs. 8 and 10). In São Lourenço, the streamflow reduction was greater
383 under the A1B scenario, whereas in Guadalupe the reduction was greater under the B1 scenario
384 (Fig. 8).

385 The decrease in sediment export caused by climate change in São Lourenço was cumulative
386 with the decrease caused by the land use change, leading to an overall reduction of 29% and 22%,
387 for scenario A1B and B1 respectively (Fig. 9). For Guadalupe, by contrast, the increase caused by
388 climate change did not added up to the increase caused by land use change. In this catchment, the

389 overall change in sediment export relative to the baseline scenario amounted to an increase of
390 222% for scenario A1B and of 5% for scenario B1 (Fig. 9).

391

392 **4 Discussion**

393

394 **4.1 Model performance**

395 Based on the criteria for model performance established by Moriasi et al. (2007), the model
396 adequately simulated monthly streamflow discharge in both catchments (Table 3). The model also
397 adequately simulated sediment export in São Lourenço, despite some underestimation in both the
398 calibration and validation periods (Table 3). This underestimation may be in part due to the method
399 of estimating sediment export, as there was not a continuous measurement of sediment
400 concentrations in this basin.

401 Monthly sediment export predictions in Guadalupe were only accurate for the validation
402 period (Table 3). However, this can be consider an artefact, since the single sediment peak during
403 the calibration period was located between two months (March and April 2013). Daily-scale model
404 errors within this relatively short time span propagate into the monthly analysis, as can be seen in
405 Fig. 6. When the evaluation is corrected for this artefact (i.e. comparing 30-day averages), the RSR
406 decreases to 0.3 and NSE increases to 0.86, indicating an accurate simulation of monthly sediments
407 in Guadalupe during the calibration period as well.

408 As the model performance statistics RSR and NSE are known to be overly sensitive to model
409 fit to peak streamflow events (Beven, 2012), a poorer performance for Guadalupe (especially for
410 sediments) would be expected compared with São Lourenço, especially at the daily scale (Table 3
411 and Figs. 5 and 6). A similar explanation can be given for the lower model performance at the daily
412 scale compared with the monthly scale, also discussed by Moriasi et al. (2007) for the SWAT model,
413 since performances conducted on monthly measurements tend to smooth out the predicted error
414 by reducing the peaks and troughs in the data.

415 SWAT was thus successfully applied to both catchments, indicating that it is a valid tool for
416 simulating the effects of climate and land use changes. Arguably, an assessment of data and model
417 uncertainty would have been important for this study since it would impact the predictions for the
418 chosen scenarios; it would also have been interesting to compare model and scenario uncertainty
419 (discussed below). Uncertainty in streamflow and especially sediment data could limit the validity
420 of the SWAT calibration (Sellami et al., 2013), but this was not quantified. The short period for data
421 collection could also limit the variability of conditions used for calibration (Lespinas et al., 2014;
422 Piras et al., 2014). However, the marked intra-annual variability, combined with the selection of a
423 drought year (2011/2012) for calibration in Guadalupe, could have helped to limit the importance
424 of this issue. In fact, Lespinas et al. (2014) found the length of the calibration period to be less
425 important than the selection of model structure (in their case, the evapotranspiration calculation
426 method) for reducing uncertainty. In this case, the use of streamflow, runoff, soil moisture and (in
427 Guadalupe) evapotranspiration data would have helped to decrease uncertainty through a multi-
428 objective calibration approach (Efstratiadis and Koutsoyiannis, 2010; Beven, 2012). Furthermore,
429 measured data was used to severely restrict the range of calibrated parameters (SOL_AWC, USLE_K,
430 ALPHA_BF and DEP_IMP in Table 2) which could have further limited parameter uncertainty (Beven,
431 2012). Finally, model structure could have contributed for uncertainty, notably due to the erosion
432 simulation method not accounting for rain-splash erosion (Arnold et al., 2011).

433

434 **4.2 Effects of climate changes**

435 The impacts of climate change scenarios on stream discharge (Fig. 8) seemed to be related to the
436 decrease in precipitation forecasted for both catchments (Fig. 10). These results agree with findings
437 from studies in other basins of the Iberian Peninsula (e.g. Lopéz-Moreno et al., 2014; Molina-
438 Navarro et al., 2014; Nunes et al., 2008, 2013; Zabaleta et al., 2014), as well as elsewhere in the
439 Mediterranean (e.g. Lespinas et al., 2014; Piras et al., 2014; Stigter et al., 2014). In these studies, a
440 decrease in precipitation due to climate changes has been identified as the main cause of reduced

441 surface water availability. In most of these basins, as in the present ones, the decrease in
442 precipitation results in a greater decrease in surface water. For example, Molina-Navarro et al.
443 (2014) estimated in the Ompóveda River (Spain) that an annual precipitation decrease of 6%
444 (scenario AB1) to 9% (scenario B1) in average would lead to a 22% (scenario A1B) to 34% (scenario
445 B1) reduction in annual streamflow.

446 Although the greater decrease in precipitation at the humid site of São Lourenço (see section
447 2.3) would suggest a more pronounced impact on streamflow, the reverse was found in the present
448 study. In São Lourenço, a larger decrease (-7 to -8%) in ET (Fig. 10) can be attributed to the large
449 decreases in the main land-cover types of vine (-9 to -11%) and maritime pine (-7 to -8%), as seen
450 in Table 6. In Guadalupe, the lower decrease in ET (-4 to -6%) is linked with lower decreases in the
451 main covers of oak (-4 to -6%) and pasture (-4 to -5%), as seen in Table 7. The differences between
452 the catchments may be that vine and maritime pine are less able to control evapotranspiration than
453 Mediterranean evergreen oaks, while annual crops benefit from warmer winters by increased
454 growth under wet conditions (Nunes and Seixas, 2011). As a result, the impacts of climate changes
455 on water yield were slightly more pronounced at Guadalupe (-14 to -18%) than in São Lourenço (-
456 13%).

457 With respect to sediment export, the 9 to 11% decrease in annual export predicted for São
458 Lourenço may be due to the decrease in precipitation predicted for this catchment. Reduction in
459 rainfall is generally linked with decreased runoff and soil erosion (Kalogeropoulos and Chalkias,
460 2013; Nunes et al., 2008; Perazzoli et al., 2013; Zabaleta et al., 2014), particularly in regions where
461 there is year round crop cover (Cerdan et al., 2010; Nunes et al., 2011). The most important land-
462 cover types in São Lourenço (i.e. vineyards and maritime pine) are permanent, and both showed a
463 decrease in erosion (Table 8). Similar results have been reported in other humid regions for climate
464 change scenarios forecasting a reduction in precipitation (Bangash et al., 2013; Khoi and Suetsugi,
465 2014; Lu et al., 2013; Mullan, 2013). In Guadalupe, on the other hand, sediment export increased
466 under both climate change scenarios, mostly due to large increases in erosion for wheat and

467 pasture (i.e. annual crops; Table 9). The increase in precipitation forecasted in winter months, which
468 is associated with the generally low vegetation cover during the cold season, increased soil erosion
469 in this catchment. This finding agrees with the results of other authors (Khoi and Suetsugi, 2014; Li
470 et al., 2012; Nunes et al., 2008). However, it should be noted that the permanent vegetation cover
471 in this catchment (i.e. oak and olive groves) showed a reduction in erosion rates (Table 9) similar to
472 the findings from the humid catchment (Table 8).

473 As discussed earlier, the uncertainty in climate scenario was not considered in this study. Two
474 greenhouse gas emission scenarios were assessed, but only one GCM and downscaling method was
475 applied. The resulting climate predictions were within the bounds simulated by the PRUDENCE
476 (Déqué et al., 2005) and ENSEMBLES projects (Van Der Linden and Mitchell, 2009), but close to the
477 lowest degree of change (see Nunes et al., 2008). A more complete assessment should consider
478 uncertainty in GCM and downscaling methods, and in particular assess the impacts of more
479 extreme climate change scenarios.

480

481 **4.3 Effects of land use changes**

482 In contrast to the climate change impacts, land use change had a minor impact on stream discharge
483 (Fig. 8). For São Lourenço, a very small increase in discharge was predicted under both scenarios,
484 despite an increase in ET (Fig. 10). This mostly was due to the expansion of corn, which is irrigated
485 and adds another source of water to the catchment. The replacement of vineyards and pastures by
486 forests and cereals also led to higher interception and transpiration, as seen in Table 6. This finding
487 agrees with previous studies examining the impact of cereals (García-Ruiz and Lana-Renault, 2011;
488 López-Vicente et al., 2013) and of forests (Jordan et al., 2014; Khoi and Suetsugi, 2014; López-
489 Moreno et al., 2014; Molina-Navarro et al., 2014; Montenegro and Ragab, 2012). However, a
490 decrease in ET in eucalypts should also be noted (Table 6) and is linked to its expansion to soils with
491 lower water holding capacity. In contrast, the higher increase in flow discharge in Guadalupe under
492 the A1B scenario was mainly related to a decrease in ET (Figs. 8 and 10), linked with the conversion

493 of pastures into sunflower plantations, since the latter is a spring crop with lower cover and water
494 demands (Table 7).

495 With respect to soil erosion, the larger decrease (-18%) in sediment export in São Lourenço
496 under scenario A1B (Fig. 9) was mainly the result of a reduction in vineyard areas (Table 4). This
497 crop type has previously been found to have the highest erosion rates (Table 8) among the cultures
498 typically cultivated in the Mediterranean basin (Cerdan et al., 2010). By contrast, the decrease
499 observed under scenario B1 (-10%) resulted from the conversion of pasture into pine plantations,
500 since forests typically have lower erosion rates (Table 8) than grasslands (e.g. Cerdan et al., 2010;
501 García-Ruiz and Lana-Renault, 2011; Nunes et al., 2011). For Guadalupe, on the other hand, the
502 replacement of pasture by sunflower (A1B scenario) led to a sharp increase in soil erosion (+257%).
503 This may be attributed to the lack of ground cover during the wet season leading to higher soil
504 losses (Table 9) than would occur with permanent vegetation cover (Cerdan et al., 2010; Nearing et
505 al., 2005; Nunes et al., 2011). For scenario B1, a considerably smaller increase in sediment export
506 (+9%) was observed in Guadalupe, largely because there was less of a conversion of pasture into
507 sunflower than in the A1B scenario (Table 5), but also because the erosion rates of sunflower and
508 wheat (which was fully replaced by sunflower in scenario B1) tend to be very similar (respectively,
509 1.34 and 1.67 tons ha⁻¹; Table 9).

510 From the results of the present study, the differences between the two catchments with
511 regards to sediment export were largely related to the growing cycle of the different crops (García-
512 Ruiz and Lana-Renault, 2011; Nearing et al., 2004). In the humid area, most crops have year-round
513 soil cover, whereas in the dry areas soils are often bare in the winter. This reduces the protection
514 of soils against rain-splash and particle detachment during the rainy season, thereby exposing the
515 soils to enhanced erosion (Cerdan et al., 2010; García-Ruiz and Lana-Renault, 2011; Nearing et al.,
516 2004, 2005; Nunes et al., 2008).

517 The land use change scenarios assumed a single societal response for each socio-economic
518 storyline, but these responses can have a high degree of uncertainty (see Stigter et al., 2015). For

519 example, an incentive for planting vineyards instead of eucalypts in São Lourenço, or olive trees
520 instead of sunflower in Guadalupe, could have led to different erosion rates. A more complete work
521 should consider different plausible land-use changes to assess a range of impacts.

522

523 **4.4 Combined effects of climate and land use changes**

524 Climate and land use changes showed off-setting effects on stream discharge and sediment export
525 at the humid catchment. In this watershed, flow discharge and sediment export were forecasted to
526 decrease, particularly under the A1B scenario (Figs. 8 and 9), as a combined effect of reduced
527 precipitation and cultivation of more soil-protective crops (Nunes et al., 2008). A different response
528 was observed for the dry catchment, as a decrease in streamflow and an increase in sediment
529 export was predicted as a result of combined climate and land use changes (Figs. 8 and 9). For
530 Guadalupe, the cultivation of less water-demanding species was not able to offset the reduction in
531 stream discharge resulting from reduced precipitation. On the other hand, the increase in sediment
532 export associated with the cultivation of highly erosion-prone crops was not aggravated by the
533 higher rainfall amounts forecasted for winter months. In fact, the combined impact of climate and
534 land use changes on soil erosion, particularly under the A1B scenario was less severe than would
535 be expected, mostly due to a decrease in erosion from sunflower under the combined scenarios
536 (from 1.44 to 1.30 tons ha⁻¹; Table 9), but also due to the decrease in olive groves. A decrease in
537 erosion under climate change for spring crops could be associated with warmer winters leading to
538 more vegetation cover in the wet season (Nunes and Seixas, 2011). Nonetheless, the high erosion
539 rates predicted for Guadalupe, which are higher than the tolerable soil erosion rates in Europe (\approx 1
540 tons ha⁻¹; Verheijen et al., 2012), might pose severe problems for soil productivity due to the
541 shallowness and poor quality of local soils (Nunes et al., 2008). The combined scenario analysis also
542 did not address the uncertainties which underlie climate and land-use scenarios. One method to
543 ensure this in a more complete work would be to adopt an uncertainty assessment framework,

544 such as the one proposed by Ludwig et al. (2010), to address uncertainty at each step of the impact
545 assessment study.

546

547 **5 Conclusions**

548 In the present work, SWAT was successfully applied to a humid and dry Mediterranean catchment,
549 demonstrating its application as a valid tool for predicting the impacts of climate and land use
550 changes on streamflow and sediment export.

551 From the integrated analysis of the effect of the two environmental stressors, climate changes
552 were predicted to have a more pronounced impact on water availability than land use changes. The
553 reverse was predicted for sediment export, which reinforces the importance of land use changes
554 for the future state of Mediterranean soils and for minimizing the indirect effects of climate
555 changes. In this case, the potential negative impact of the expansion of sunflower cultivation for
556 soil protection in the dry site is stressed, suggesting alternative land use policies with equivalent
557 economic value, such as the expansion of olive groves.

558 The results of this study stress the importance of present-day land cover for climate change
559 impacts. The humid catchment, with permanent vegetation cover, is expected to experience less
560 negative impacts on available water resources and even an increase of soil protection. The dry
561 catchment by contrast, which has either drought-adapted permanent vegetation or annual winter
562 crops, is expected to experience larger negative impacts on both water resources and soil
563 protection. While vegetation cover is an indirect function of climate, these results also point to land
564 use policies that could help mitigate the impacts of climate change on soil degradation, e.g. by
565 promoting the maintenance of vegetation with permanent cover, such as pasture, olive groves, or
566 natural shrublands.

567 This study did not address scenario uncertainty, i.e. from greenhouse gas emission, selection
568 of climate model and downscaling method, and selection of socio-economic scenario, since the
569 relatively limited objectives only required a small number of plausible scenarios. However, a

570 complete assessment of potential climate change impacts should take these uncertainties into
571 account, especially by considering a large range of GCM/RCM combinations and of socio-economic
572 responses.

573 From the present work, it becomes evident that an integrated approach combining the effects
574 of climate and land cover change is crucial for a realistic evaluation of the future state of natural
575 resources. Despite being a starting point towards a better understanding of the direct and indirect
576 impacts of climate change on Mediterranean watersheds, this study provides important
577 information that can be useful for decision-makers to design adaptive measures to climate changes.
578 Future work should address the range of foreseeable scenarios for the study area, to take into
579 account the uncertainty inherent to climate and land use change predictions.

580

581 **Acknowledgments**

582

583 This study was funded by the European Regional Development Fund (through the Competitiveness
584 Factors Operational Programme – COMPETE), the European Social Fund (through Human Potential
585 Operational Programme) and the Portuguese Republic (through the Portuguese Foundation for
586 Science and Technology – FCT), under the scope of the PEst (PEst-C/MAR/LA0017/2013), VITAQUA
587 (PTDC/AAC-AMB/112438/2009 and FCOMP-01-0124-FEDER-013912) and ERLAND (PTDC/AAC-
588 AMB/100520/2008 and FCOMP-01-0124-FEDER-008534) Projects. Serpa D. was a recipient of a
589 grant from FCT (SFRH/BPD/92650/2013) as well as Abrantes N. (SFRH/BPD/84833/2012) and Nunes
590 J. P. (SFRH/BPD/39721/2007 and SFRH/BPD/87571/2012). The authors would also like to thank
591 MSc. Daniel Hawtree for the revision of the English language and to two anonymous reviewers for
592 their valuable comments on the manuscript.

593

594 **References**

595

596 Arnold JG, Kiniry JR, Srinivasan R, Williams JR, Haney EB, Neitsch SL. Soil and Water Assessment Tool
597 theoretical documentation, Version 2009, 2011. Texas: Texas Water Resources Institute technical
598 report No 365; 2011.

599

600 Arnold JG, Srinivasan R, Muttiah RS, Williams JR. 1998. Large area hydrologic modeling and
601 assessment – Part 1: Model development. *Journal of the American Water Resources Association*
602 34, 73–89.

603

604 Bangash RF, Passuello A, Sanchez-Canales M, Terrado M, López A, Elorza FJ, Ziv G, Acuña V,
605 Schuhmacher M. 2013. Ecosystem services in Mediterranean river basin: Climate change impact on
606 water provisioning and erosion control. *Science of the Total Environment* 458–460, 246–255.

607

608 Beguería S, López-Moreno JI, Lorente A, Seeger M, García-Ruiz JM. 2003. Assessing the effect of
609 climate oscillations and land-use changes on streamflow in the Central Spanish Pyrenees. *Ambio*
610 32, 283–286.

611

612 Beven KJ. *Rainfall-Runoff Modelling: The Primer*. Hoboken: Wiley-Blackwell; 2012.

613

614 Camacho-B SE, Hall AE, Kaufmann MR. 1974. Efficiency and Regulation of Water Transport in Some
615 Woody and Herbaceous Species. *Plant Physiology* 54, 169–172.

616

617 Cardoso JC, Bessa MT, Marado MB. 1973. Carta dos solos de Portugal – 1:1.000.000. *Agronomia*
618 *Lusitana* 33 (1-4), 481–602.

619

620 Cardoso JVJC. *Os solos de Portugal, sua classificação, caracterização e génese: 1- a sul do rio Tejo*.
621 Lisbon: General-Directorate for Agricultural Services; 1965.

622

623 Cerdan O, Govers G, Le Bissonnais Y, Van Oost K, Poesen J , Saby N, Gobin A, Vacca A, Quinton J,
624 Auerswald K, Klik A, Kwaad FJPM, Raclot D, Ionita I, Rejman J, Rousseva S, Muxart T, Roxo MJ, Dostal
625 T. 2010. Rates and spatial variations of soil erosion in Europe: A study based on erosion plot data.
626 *Geomorphology* 122, 167–177.

627

628 Compo GP, Whitaker JS, Sardeshmukh PD, Matsui N, Allan RJ, Yin X, Gleason BE, Vose RS, Rutledge
629 G, Bessemoulin P, Brönnimann S, Brunet M, Crouthamel RI, Grant AN, Groisman PY, Jones PD, Kruk
630 M, Kruger AC, Marshall GJ, Maugeri M, Mok HY, Nordli Ø, Ross TF, Trigo RM, Wang XL, Woodruff
631 SD, Worley SJ. 2011. The Twentieth Century Reanalysis Project. *Quarterly Journal of the Royal
632 Meteorological Society* 137, 1–28.

633

634 Corte-Real J, Qian B, Xu H. 1998. Regional climate change in Portugal: precipitation variability
635 associated with large-scale atmospheric circulation. *International Journal of Climatology* 18, 619–
636 635.

637

638 De Girolamo AM, Lo Porto A. 2012. Land use scenario development as a tool for watershed
639 management within the Rio Mannu Basin. *Land Use Policy* 29, 691–701.

640

641 Deidda R, Marrocu M, Caroletti G, Pusceddu G, Langousis A, Lucarini V, Puliga M, Speranza A. 2013.
642 Regional climate models' performance in representing precipitation and temperature over selected
643 Mediterranean areas. *Hydrology and Earth System Sciences* 17, 5041–5059.

644

645 Déqué M, Jones RG, Wild M, Giorgi F, Christensen JH, Hassell DC, Vidale PL, Rockel B, Jacob D,
646 Kjellström E, de Castro M, Kucharski F, van den Hurk B. 2005. Global high resolution versus Limited

647 Area Model climate change projections over Europe: quantifying confidence level from PRUDENCE
648 results. *Climate Dynamics* 25, 653–670.

649

650 DGADR, Direcção-Geral de Agricultura e Desenvolvimento Rural. 2013. Solos, cartografia e
651 informação geográfica. Available online at: [http://www.dgadr.mamaot.pt/cartografia/cartas-solos-](http://www.dgadr.mamaot.pt/cartografia/cartas-solos-cap-uso-digital)
652 [cap-uso-digital](http://www.dgadr.mamaot.pt/cartografia/cartas-solos-cap-uso-digital). Last accessed on February 2013.

653

654 Efstratiadis A, Koutsoyiannis D. 2010. One decade of multi-objective calibration approaches in
655 hydrological modelling: a review. *Hydrological Sciences Journal* 55, 58–78.

656

657 Gallart F, Llorens P. 2004. Observations on land cover changes and water resources in the
658 headwaters of the Ebro catchment, Iberian Peninsula. *Physics and Chemistry of the Earth* 29, 769–
659 773.

660

661 García-Ruiz JM. 2010. The effects of land uses on soil erosion in Spain: a review. *Catena* 81, 1–11.

662

663 García-Ruiz JM, Lana-Renault N. 2011. Hydrological and erosive consequences of farmland
664 abandonment in Europe, with special reference to the Mediterranean region – A review.
665 *Agriculture, Ecosystems and Environment* 140, 317–338.

666

667 García-Ruiz JM, Nadal-Romero E, Lana-Renault N, Beguería S. 2013. Erosion in Mediterranean
668 landscapes: Changes and future challenges. *Geomorphology* 198, 20–36.

669

670 Gilmanov TG, Soussana JF, Aires L, Allard V, Ammann C, Balzarolo M, Barcza Z, Bernhofer C,
671 Campbell CL, Cernusca A, Cescatti A, Clifton-Brown J, Dirks BOM, Dore S, Eugster W, Fuhrer J,

672 Gimeno C, Gruenwald T, Haszpra L, Hensen A, Ibrom A, Jacobs AFG, Jones MB, Lanigan G, Laurila T,
673 Lohila A, Manca G, Marcolla B, Nagy Z, Pilegaard K, Pinter K, Pio C, Raschi A, Rogiers N, Sanz MJ,
674 Stefani P, Sutton M, Tuba Z, Valentini R, Williams ML, Wohlfahrt G. 2007. Partitioning European
675 grassland net ecosystem CO₂ exchange into gross primary productivity and ecosystem respiration
676 using light response function analysis, *Agriculture, Ecosystems and Environment* 121, 9–120.

677

678 Graffin SR, Rosenzweig CR, Xing X, Yetman G. Downscaling and geo-spatial gridding of socio-
679 economic projections from the IPCC Special Report on Emissions Scenarios (SRES). Columbia:
680 CIESIN, Center for Climate Systems Research, Columbia University; 2004.

681

682 Hargreaves GL, Hargreaves GH, Riley JP. 1985. Agricultural benefits for Senegal River Basin. *Journal*
683 *of Irrigation and Drainage Engineering* 111, 113–124.

684

685 Hoque YM, Raj C, Hantush MM, Chaubey I, Govindaraju RS. 2014. How Do Land-Use and Climate
686 Change Affect Watershed Health? A Scenario-Based Analysis. *Water Quality, Exposure and Health*
687 6, 19–33.

688

689 IGeoE, Instituto Geográfico do Exército. 1990. Carta de ocupação do solo COS 90. Available online
690 at: http://dgterritorio.pt/e-IGEO/egeo_downloads.htm. Last accessed on February 2013.

691

692 IGeoE, Instituto Geográfico do Exército. 2007. Carta de ocupação do solo COS 2007. Available online
693 at: http://dgterritorio.pt/e-IGEO/egeo_downloads.htm. Last accessed on February 2013.

694

695 IGeoE, Instituto Geográfico do Exército. 2013. Modelo Digital do Terreno para Portugal. Available
696 online at: <http://www.igeoe.pt/index.php?id=39>. Last accessed on February 2013.

697

698 INIA-LQARS, Instituto Nacional de Investigação Agrária. Manual de fertilização das culturas. Lisbon:
699 Ministério da Agricultura, do Desenvolvimento Rural e das Pescas; 2000

700

701 IPCC, Intergovernmental Panel on Climate Change. Contribution of Working Group II to the Fourth
702 Assessment Report of the Intergovernmental Panel on Climate Change. Parry ML, Canziani OF,
703 Palutikof JP, van der Linden PJ, Hanson CE, editors. Cambridge, New York: Cambridge University
704 Press; 2007.

705

706 IPCC, Intergovernmental Panel on Climate Change. Climate Change 2013: The Physical Science
707 Basis. Contribution of Working Group I to the Fifth Assessment Report of the Intergovernmental
708 Panel on Climate Change. Stocker TF, Qin D, Plattner G-K, Tignor M, Allen SK, Boschung J, Nauels A,
709 Xia Y, Bex V, Midgley PM, editors. Cambridge, New York: Cambridge University Press; 2013.

710

711 Jacinto R, Cruz MJ, Santos FD. 2013. Development of water use scenarios as a tool for adaptation
712 to climate change. *Drinking Water Engineering and Science* 6, 61–68.

713

714 Jones N, Graaff J, Rodrigo I, Duarte F. 2011. Historical review of land use changes in Portugal (before
715 and after EU integration in 1986) and their implications for land degradation and conservation, with
716 a focus on Centro and Alentejo regions. *Applied Geography* 31, 1036–1048.

717

718 Jordan YC, Ghulam A, Hartling S. 2014. Traits of surface water pollution under climate and land use
719 changes: A remote sensing and hydrological modeling approach. *Earth-Science Reviews* 128, 181–
720 195.

721

722 Kalantari Z, Lyon SW, Folkeson L, French HK, Stolte J, Jansson P-E, Sassner M. 2014. Quantifying the
723 hydrological impact of simulated changes in land use on peak discharge in a small catchment.
724 Science of the Total Environment 466–467,741–754.
725

726 Kalogeropoulos K, Chalkias C. 2013. Modelling the impacts of climate change on surface runoff in
727 small Mediterranean catchments: empirical evidence from Greece. Water and Environment Journal
728 27, 505–513.
729

730 Khoi DN, Suetsugi T. 2014. The responses of hydrological processes and sediment yield to land-use
731 and climate change in the Be River Catchment, Vietnam. Hydrological Processes 28, 640–652.
732

733 Kilsby CG, Tellier SS, Fowler HJ, Howels TR. 2007. Hydrological impacts of climate change on the
734 Tejo and Guadiana Rivers. Hydrology and Earth Systems Science 11, 1175–1189.
735

736 Lespinas F, Ludwig W, Heussner S. 2014. Hydrological and climatic uncertainties associated with
737 modeling the impact of climate change on water resources of small Mediterranean coastal rivers.
738 Journal of Hydrology 511, 403–422.
739

740 Li D, Tian Y, Liu C, Hao F. 2004. Impact of land-cover and climate changes on runoff of the source
741 regions of the Yellow River. Journal of Geographical Sciences 14, 330-338.
742

743 Li H, Zhang Y, Vaze J, Wang B. 2012. Separating effects of vegetation change and climate variability
744 using hydrological modelling and sensitivity-based approaches. Journal of Hydrology 420–421, 403–
745 418.
746

747 Li Z, Liu W-Z, Zhang X-C, Zheng F-L. 2009. Impacts of land use change and climate variability on
748 hydrology in an agricultural catchment on the Loess Plateau of China. *Journal of Hydrology* 377, 35–
749 42.

750

751 López-Moreno JI, Vicente-Serrano SM, Moran-Tejeda E, Zabalza J, Lorenzo-Lacruz J, García-Ruiz JM.
752 2011. Impact of climate evolution and land use changes on water yield in the Ebro basin.
753 *Hydrological Earth System Sciences* 15, 311–22.

754

755 López-Moreno JI, Zabalza J, Vicente-Serrano SM, Revuelto J, Gilaberte M, Azorin-Molina C, Morán-
756 Tejeda E, García-Ruiz JM, Tague C. 2014. Impact of climate and land use change on water availability
757 and reservoir management: Scenarios in the Upper Aragón River, Spanish Pyrenees. *Science of the*
758 *Total Environment* 493, 1222–1231.

759

760 López-Vicente M, Poesen J, Navas A, Gaspar L. 2013. Predicting runoff and sediment connectivity
761 and soil erosion by water for different land use scenarios in the Spanish Pre-Pyrenees. *Catena* 102,
762 62–73.

763

764 Lu XX, Ran LS, Liu S, Jiang T, Zhang SR, Wang JJ. 2013. Sediment loads response to climate change:
765 A preliminary study of eight large Chinese rivers. *International Journal of Sediment Research* 28, 0–
766 14.

767

768 Ludwig R, Soddu A, Duttmann R, Baghdadi N, Benabdallah S, Deidda R, Marrocu M, Strunz G,
769 Wendland F, Engin G, Paniconi C, Prettenthaler F, Lajeunesse I, Afifi S, Cassiani G, Bellin A, Mabrouk
770 B, Bach H, Ammerl T. 2010. Climate induced changes on the hydrology of Mediterranean basins - A
771 research concept to reduce uncertainty and quantify risk. *Fresenius Environmental Bulletin* 19.

772

773 Luo Y, Ficklin DL, Liu X, Zhang M. 2013. Assessment of climate change impacts on hydrology and
774 water quality with a watershed modeling approach. *Science of the Total Environment* 450–451, 72–
775 82.

776

777 Majone B, Villa F, Deidda R, Bellin A. 2015. Impact of climate change and water use policies on
778 hydropower potential in the south-eastern Alpine region. *Science of The Total Environment*, in
779 press. DOI: 10.1016/j.scitotenv.2015.05.009.

780

781 Mango LM, Melesse AM, McClain ME, Gann D, Setegn SG. 2011. Land use and climate change
782 impacts on the hydrology of the upper Mara River Basin, Kenya: results of a modeling study to
783 support better resource management. *Hydrological Earth System Sciences* 15, 2245–2258.

784

785 Maraun D, Wetterhall F, Ireson AM, Chandler RE, Kendon EJ, Widmann M, Brienen S, Rust HW,
786 Sauter T, Themeßl M, Venema VKC, Chun KP, Goodess CM, Jones RG, Onof C, Vrac M, Thiele-Eich I.
787 2010. Precipitation downscaling under climate change: Recent developments to bridge the gap
788 between dynamical models and the end user. *Reviews of Geophysics* 48, RG3003.

789

790 McMillan H, Freer J, Pappenberger F, Krueger T, Clark M. 2010. Impacts of uncertain river flow data
791 on rainfall-runoff model calibration and discharge predictions. *Hydrological Processes* 24, 1270–
792 1284.

793

794 Middleton N, Thomas D. *World Atlas of Desertification*. London: United Nations Environment
795 Program, UNEP; 1997.

796

797 Milly PCD, Dunne KA, Vecchia AV. 2005. Global pattern of trends in stream flow and water
798 availability in a changing climate. *Nature* 438, 347–50.

799

800 Molina-Navarro E, Trolle D, Martinez-Perez S, Sastre-Merlin A, Jeppesen E. 2014. Hydrological and
801 water quality impact assessment of a Mediterranean limno-reservoir under climate change and
802 land use management scenarios. *Journal of Hydrology* 509, 354–366.

803

804 Montenegro S, Ragab R. 2012. Impact of possible climate and land use changes in the semi arid
805 regions: A case study from North Eastern Brazil. *Journal of Hydrology* 434–435, 55–68.

806

807 Moreira F, Rego FC, Ferreira PG. 2001. Temporal (1958–1995) pattern of change in a cultural
808 landscape of northwestern Portugal: implications for fire occurrence. *Landscape Ecology* 16, 557–
809 567.

810

811 Moriasi DN, Arnold JG, Van Liew MW, Bingner RL, Harmel RD, Veith TL. 2007. Model evaluation
812 guidelines for systematic quantification of accuracy in watershed simulations. *American Society of
813 Agricultural and Biological Engineers* 50, 885–900.

814

815 Mourato S, Moreira M, Corte-Real J. 2015. Water resources impact assessment under climate
816 change scenarios in Mediterranean watersheds. *Water Resources Management*, in press. DOI:
817 10.1007/s11269-015-0947-5.

818

819 Mullan D. 2013. Soil erosion under the impacts of future climate change: Assessing the statistical
820 significance of future changes and the potential on-site and off-site problems. *Catena* 109, 234–
821 246.

822

823 Nakićenović N, Swart R. Special Report on Emissions Scenarios. A Special Report of Working Group
824 III of the Intergovernmental Panel on Climate Change. Cambridge: Cambridge University Press;
825 2000.

826

827 NCDC, National Climatic Data Center of the National Oceanic and Atmospheric Administration.
828 2014. Global Summary of the Day. Available online at: <http://www.ncdc.noaa.gov/>. Last accessed
829 on June 2014.

830

831 Nearing MA, Jetten V, Baffaut C, Cerdan O, Couturier A, Hernandez M, Le Bissonnais Y, Nichols MH,
832 Nunes JP, Renschler CS, Souchère V, van Oost K. 2005. Modeling response of soil erosion and runoff
833 to changes in precipitation and cover. *Catena* 61, 131–154.

834

835 Nearing MA, Pruski FF, O'Neal MR. 2004. Expected climate change impacts on soil erosion rates: a
836 review. *Journal of Soil and Water Conservation* 59, 43–50.

837

838 Neitsch SL, Arnold JG, Kiniry JR, Williams JR. Soil and Water Assessment Tool theoretical
839 documentation. Version 2009. Texas: Texas Water Resources Institute Technical Report No. 406,
840 Texas A&M University System; 2011.

841

842 Neitsch SL, Arnold JG, Kiniry JR, Williams JR, Kiniry KW. Soil and Water Assessment Tool theoretical
843 documentation. Texas: Texas Water Resources Institute, TWRI report TR-191; 2002.

844

845 Nunes AN, Almeida AC, Coelho COA. 2011. Impacts of land use and cover type on runoff and soil
846 erosion in a marginal area of Portugal. *Applied Geography* 31, 687–699.

847

848 Nunes AN, Coelho COA, Almeida AC, Figueiredo A. 2010. Soil erosion and hydrological response to
849 land abandonment in a central Inland area of Portugal. *Land Degradation and Development* 21,
850 260–273.

851

852 Nunes JP, Nearing MA. Modelling impacts of climatic change: case studies using the new generation
853 of erosion models. In: Morgan RPC, Nearing MA, editors. *Handbook of Erosion Modelling*. Oxford:
854 Wiley-Blackwell; 2011. p. 289–312.

855

856 Nunes JP, Seixas J. Modelling the impacts of climate change on water balance and agricultural and
857 forestry productivity in southern Portugal using SWAT. In: Shukla MK, editor. *Soil Hydrology, Land-
858 Use and Agriculture: Measurement and Modelling*. Wallingford: CABI; 2011. p. 366–383.

859

860 Nunes JP, Seixas J, Keizer JJ. 2013. Modeling the response of within-storm runoff and erosion
861 dynamics to climate change in two Mediterranean watersheds: A multi-model, multi-scale
862 approach to scenario design and analysis. *Catena* 102, 27–39.

863

864 Nunes JP, Seixas J, Pacheco NR. 2008. Vulnerability of water resources, vegetation productivity and
865 soil erosion to climate change in Mediterranean watersheds. *Hydrological Processes* 22, 3115–
866 3134.

867

868 Paço TA, David TS, Henriques MO, Pereira JS, Valente F, Banza J, Pereira FL, Pinto C, David JS. 2009.
869 Evapotranspiration from a Mediterranean evergreen oak savannah: The role of trees and pasture.
870 *Journal of Hydrology* 369, 98–106.

871

872 Perazzoli M, Pinheiro A, Kaufmann V. 2013. Assessing the impact of climate change scenarios on
873 water resources in southern Brazil. *Hydrological Sciences Journal* 58, 77–87.

874

875 Reichstein M, Rey A, Freibauer A, Tenhunen J, Valentini R, Banza J, Casals P, Cheng YF, Grunzweig
876 JM, Irvine J, Joffre R, Law BE, Loustau D, Miglietta F, Oechel W, Ourcival JM, Pereira JS, Peressotti
877 A, Ponti F, Qi Y, Rambal S, Rayment M, Rom J. 2003. Modeling temporal and large-scale spatial
878 variability of soil respiration from soil water availability, temperature and vegetation productivity
879 indices. *Global Biogeochemical Cycles* 17, 1104.

880

881 Piras M, Mascaro G, Deidda R, Vivoni ER. 2014. Quantification of hydrologic impacts of climate
882 change in a Mediterranean basin in Sardinia, Italy, through high-resolution simulations. *Hydrology
883 and Earth System Sciences* 18, 5201–5217.

884

885 Roeckner E, Bäuml G, Bonaventura L, Brokopf R, Esch M, Giorgetta M, Hagemann S, Kirchner I,
886 Kornblueh L, Manzini E, Rhodin A, Schlese U, Schilzweida U, Tompkins A. The atmosphere general
887 circulation model ECHAM5, part I: model description. Hamburg: Max–Planck Institute for
888 Meteorology - Report no. 349; 2003.

889

890 Rounsevell MDA, Reginster I, Araujo MB, Carter TR, Dendoncker N, Ewert F, House JI, Kankaanpaa
891 S, Leemans R, Metzger MJ, Schmit C, Smith P, Tuck G. 2006. A coherent set of future land use change
892 scenarios for Europe. *Agriculture, Ecosystems and Environment* 114, 57–68.

893

894 SCS, Soil Conservation Service. *National Engineering Handbook, Section 4: Hydrology.*
895 Washington D.C.: Soil Conservation Service, USDA; 1985.

896

897 Sellami H, La Jeunesse I, Benabdallah S, Vanclooster M. 2013. Parameter and rating curve
898 uncertainty propagation analysis of the SWAT model for two small Mediterranean catchments.
899 *Hydrological Sciences Journal* 58, 1635–1657.

900

901 SNIRH, Sistema Nacional de Informação de Recursos Hídricos. 2014a. Dados de Base. Available
902 online at: snirh.apambiente.pt. Last accessed on May 2014.

903

904 SNIRH, Sistema Nacional de Informação de Recursos Hídricos. 2014b. Atlas da Água. Available
905 online at: geo.snirh.pt/AtlasAgua. Last accessed on January 2014.

906

907 Stigter TY, Nunes JP, Pisani B, Fakir Y, Hugman R, Li Y, Tomé S, Ribeiro L, Samper J, Oliveira R,
908 Monteiro JP, Silva A, Tavares PCF, Shapouri M, Cancela da Fonseca L, Yacoubi-Khebiza M, El Himer
909 H. 2014. Comparative assessment of climate change impacts on coastal groundwater resources and
910 dependent ecosystems in the Mediterranean. *Regional Environmental Change* 14 (suppl. 1), 41–56.

911

912 Stigter TY, Varanda M, Bento S, Nunes JP, Hugman R. 2015. Combined Assessment of Climate
913 Change and Socio-Economic Development as Drivers of Freshwater Availability in the South of
914 Portugal. *Water Resources Management*, *in press*. DOI: 10.1007/s11269-015-0994-y.

915

916 Svanidze GG. *Mathematical Modeling of Hydrologic Series*. Colorado: Water Resources
917 Publications; 1977.

918

919 SWAT Database. 2014. Literature Database for peer-Reviewed Journal Articles. Available online at:
920 https://www.card.iastate.edu/swat_articles/. Last accessed on December 2014.

921

922 Tavares AO, Pato RL, Magalhães MC. 2012. Spatial and temporal land use change and occupation
923 over the last half century in a peri-urban area. *Applied Geography* 34, 432–444.

924

925 Van Der Linden P, Mitchell JFB. ENSEMBLES: Climate Change and its Impacts: Summary of research
926 and results from the ENSEMBLES project. Exeter: Met Office Hadley Centre; 2009.
927

928 Vanmaercke M, Poesen J, Verstraeten G, De Vewnte J, Ocakoglu F. 2011. Sediment yield in Europe:
929 spatial patterns and scale dependency. *Geomorphology* 130, 142–161.
930

931 Veiga SMF. 2013. RELATÓRIO: Downscaling de Cenários Climáticos Futuros -Task 4, University of
932 Évora. Available online at: [https://www.dropbox.com/s/rq0uaatvre1pu1w/ERLAND_2013-](https://www.dropbox.com/s/rq0uaatvre1pu1w/ERLAND_2013-05_ICAAM-UE_SV_relatorio_FINAL.pdf)
933 [05_ICAAM-UE_SV_relatorio_FINAL.pdf](https://www.dropbox.com/s/rq0uaatvre1pu1w/ERLAND_2013-05_ICAAM-UE_SV_relatorio_FINAL.pdf). Last accessed on June 2015.
934

935 Verburg PH, Schulp CJE, Witte NVA. 2006. Downscaling of land use change scenarios to assess the
936 dynamics of European landscapes. *Agriculture, Ecosystems & Environment* 114, 39–56.
937

938 Verheijen FGA, Jones RJA, Rickson RJ, Smith CJ, Bastos AC, Nunes JP, Keizer JJ. 2012. Concise
939 overview of European soil erosion research and evaluation. *Acta Agriculturae Scandinavica, Section*
940 *B -Soil & Plant Science* 62, 185–190.
941

942 Wilson CO, Weng Q. 2011. Simulating the impacts of future land use and climate changes on surface
943 water quality in the Des Plaines River watershed, Chicago Metropolitan Statistical Area, Illinois.
944 *Science of the Total Environment* 409, 4387–4405.
945

946 Xu C-Y, Singh VP. 2004. Review on Regional Water Resources Assessment Models under Stationary
947 and Changing Climate. *Water Resources Management* 18, 591–612.
948

949 Zabaleta A, Meaurio M, Ruiz E, Antigüedad I. 2014. Simulation climate change impact on runoff and
950 sediment yield in a small watershed in the Basque Country, Northern Spain. Journal of
951 Environmental Quality 43, 235–245.

952

953 **Figure captions**

954

955 **Fig. 1.** Map of Portugal showing the location of the study sites; and the UNEP aridity Index
956 (Middleton and Thomas, 1997), calculated using spatial datasets for long-term average rainfall and
957 potential evapotranspiration (SNIRH, 2014b).

958

959 **Fig. 2.** Soil, land use and slope classes defined for São Lourenço.

960

961 **Fig. 3.** Soil, land use and slope classes defined for Guadalupe.

962

963 **Fig. 4.** Flowchart of the modelling work.

964

965 **Fig. 5.** Predicted and measured daily streamflow (*top*) and sediment export (*bottom*) at the São
966 Lourenço catchment, for the calibration and validation periods.

967

968 **Fig. 6.** Predicted and measured monthly streamflow (*top*) and sediment export (*bottom*) at the
969 Guadalupe catchment, for the calibration and validation periods.

970

971 **Fig. 7.** Average monthly temperature and precipitation for the baseline scenario (1971-2000) and
972 the A1B and B1 future emission scenarios (2071-2100), in the São Lourenço and Guadalupe
973 catchments.

974

975 **Fig. 8.** Average annual (\pm standard deviation) stream discharge under different scenarios of climate,
976 land use and combined climate and land use changes, in the São Lourenço and Guadalupe
977 catchment.

978

979 **Fig. 9.** Average annual (\pm standard deviation) sediment export under different scenarios of climate,
980 land use and combined climate and land use changes, in the São Lourenço and Guadalupe
981 catchment.

982

983 **Fig. 10.** Impacts of climate, land use and combined climate and land use change scenarios on the
984 water balance of the São Lourenço and Guadalupe catchments. ET – actual evapotranspiration.

985

986

987

988

989

990

991

992

993

994

995

996

997

998

999

1000

1001 **Tables**

1002

1003 **Table 1.** Input data for SWAT application to São Lourenço and Guadalupe.

Data type	Description	Source
Topography	Digital Elevation Model (10 m)	IGeoE (2013) ^{1,2}
Soils	Soil map (1:25000)	DGADR (2013) ^{1,2}
Land use	Land use/cover classification map (1:25000)	IGeoE (1990, 2007) ^{1,2}
Hydrography	Daily streamflow and baseflow data and stage discharge curves	Field data ^{1,2}
Meteorology	Daily precipitation, maximum and minimum temperatures, solar radiation, relative humidity and wind speed	Field data ^{1,2} , SNIRH (2014a) ¹ , NCDC (2014) ¹

1004 ¹ São Lourenço; ² Guadalupe

1005

1006

1007

1008

1009

1010

1011

1012

1013

1014

1015

1016

1017

1018

1019 **Table 2.** Calibrated SWAT parameters.

Parameter	Description	Units
SOL_AWC	Available water capacity of the soil layer	mm H ₂ O/ mm
USLE_K	USLE equation soil erodibility factor	-
USLE_C	Minimum value of USLE C factor applicable to the land cover	-
RSDCO_PL	Plant residue decomposition factor	fraction
GW_DELAY	Groundwater delay	days
ALPHA_BF	Baseflow alpha factor	days ⁻¹
GWQ_MIN	Threshold depth of water in the shallow aquifer required for return flow to occur	mm H ₂ O
GW_REVAP	Groundwater re-evaporation coefficient	fraction
RCHRG_DP	Deep aquifer percolation fraction	fraction
ESCO	Soil evaporation compensation factor	-
EPCO	Plant uptake compensation factor	-
DEP_IMP	Depth to impervious layer for modelling perched water tables	mm

1020

1021

1022

1023

1024

1025

1026

1027

1028

1029

1030

1031

1032

1033

1034 **Table 3.** Model performance regarding streamflow and sediment export at the São Lourenço and
 1035 Guadalupe catchment, for the calibration and validation periods. NSE – Nash-Sutcliffe coefficient;
 1036 RSR – ratio between the Root Mean Square Error and the sample standard deviation; PBIAS –
 1037 percent of bias.

Variable	Catchment	Data	Period	NSE	RSR	PBIAS
Streamflow	São Lourenço	Daily	Calibration	0.83	0.41	0.44
			Validation	0.84	0.40	-3.34
		Monthly	Calibration	0.92	0.27	0.44
			Validation	0.97	0.15	-3.34
	Guadalupe	Daily	Calibration	0.56	0.66	1.14
			Validation	0.31	0.83	6.96
		Monthly	Calibration	0.86	0.36	0.87
			Validation	0.83	0.40	6.68
Sediment export	São Lourenço	Daily	Calibration	0.60	0.63	46.53
			Validation	0.58	0.66	35.94
		Monthly	Calibration	0.70	0.52	28.36
			Validation	0.65	0.56	31.52
	Guadalupe	Daily	Calibration	-1.73	1.65	-5.75
			Validation	-7.74	2.95	-21.86
		Monthly	Calibration	-0.37	1.13	-5.74
			Validation	0.73	0.51	-22.66

1038

1039

1040

1041

1042

1043

1044

1045

1046 **Table 4.** Present and predicted future land cover in the São Lourenço catchment.

Land use	SWAT code	Present		Scenario A1B		Scenario B1	
		Area (ha)	%	Area (ha)	%	Area (ha)	%
Vineyards	VINE	272.6	43.9	230.4 ^a	37.1	272.6	43.9
Maritime pine	MPIN	164.3	26.5	164.3	26.5	193.4	31.2
Annual crops							
Corn	CORN	74.9	12.1	147.9	23.9	110.2	17.8
Potato	POTA	17.6	2.8	0.0 ^b	0.0	0.0 ^b	0.0
Pasture	WPAS	17.6	2.8	0.0 ^b	0.0	0.0 ^b	0.0
Urban area	URHD	28.5	4.6	28.5	4.6	28.5	4.6
Permanent	PAST	18.5	3.0	0.0 ^c	0.0	0.0 ^d	0.0
Eucalypt	EUCP	16.7	2.7	48.9	7.9	16.7	2.7
Mixed forests	MIXF	9.6	1.5	0.0 ^e	0.0	0.0 ^f	0.0

1047 ^a Vineyards partially converted into corn and eucalypt plantations; ^b potato and pastures converted
1048 into corn; ^c permanent pastures converted into eucalypt; ^d permanent pastures converted into
1049 maritime pine; ^d mixed forests converted into eucalypt plantations; ^d mixed forests converted into
1050 maritime pine plantations.

1051

1052

1053

1054

1055

1056

1057

1058

1059

1060

1061

1062 **Table 5.** Present and predicted future land cover in the Guadalupe catchment.

Land use	SWAT code	Present		Scenario A1B		Scenario B1	
		Area (ha)	%	Area (ha)	%	Area (ha)	%
Cork/holm oak	FRSS	197.9	44.0	197.9	44.0	197.9	44.0
Annual crops (Wheat)	WCRL	48.1	10.7	0.0 ^a	0.0	0.0 ^a	0.0
Pasture	WPAS	190.4	42.4	25.6 ^{b, c}	5.7	107.7 ^c	24.0
Olive groves	OLVG	11.7	2.6	11.7	2.6	11.7	2.6
Urban	URMD	1.3	0.3	1.3	0.3	1.3	0.3
Sunflower	SUNF	-	-	130.2 ^{a, b}	29.0	48.1 ^a	10.7
Shrublands	SHRM	-	-	82.7 ^c	18.4	82.7 ^c	18.4

1063 ^a Annual crops converted into sunflower; ^b pastures under lower-density oaks (30-50%; Fig. 3)
 1064 converted into sunflower; ^c pastures under higher-density oaks (>50%; Fig. 3) converted into
 1065 shrublands.

1066

1067

1068

1069

1070

1071

1072

1073

1074

1075

1076

1077

1078 **Table 6.** Average actual evapotranspiration (ET; mm y⁻¹) for the São Lourenço crops, under different
 1079 climate and land use scenarios. VINE – Vineyards; MPIN – Maritime pine; POTA – Potato; WPAS –
 1080 Pasture; PAST – Permanent pasture; EUCP – Eucalypt; MIXF – Mixed forests.

Scenarios	Precipitation (mm)	ET (mm y ⁻¹)							
		VINE	MPIN	CORN	POTA	WPAS	PAST	EUCP	MIXF
Baseline	1064.3	478.0	462.5	749.9	676.5	516.7	531.7	690.1	600.6
A1B_Climate	940.0	432.8	428.7	729.8	668.1	473.8	489.4	634.7	543.6
B1_Climate	939.5	427.4	427.7	736.9	670.5	468.8	483.1	624.9	535.8
A1B_Land use	1064.3	470.1	462.5	750.2	-	-	-	617.0	-
B1_Land use	1064.3	478.0	461.2	748.8	-	-	-	690.1	-
A1B_Climate+Land use	940.0	425.1	428.7	730.5	-	-	-	560.9	-
B1_Climate+Land use	939.5	427.4	426.8	736.2	-	-	-	624.9	-

1081

1082

1083

1084

1085

1086

1087

1088

1089

1090

1091

1092

1093

1094

1095

1096 **Table 7.** Average actual evapotranspiration (ET; mm y⁻¹) for the Guadalupe crops, under different
 1097 climate and land use scenarios. FRSS – Cork/holm oak; SHRM – Mediterranean shrublands; WCRL –
 1098 Wheat; WPAS – Pasture; OLVG – Olive groves; SUNF – Sunflower.

Scenarios	Precipitation		ET (mm y ⁻¹)				
	(mm)	FRSS	SHRM	WCRL	WPAS	OLVG	SUNF
Baseline	333.0	357.4	-	366.6	362.7	386.3	-
A1B_Climate	306.3	337.2	-	347.4	343.6	363.3	-
B1_Climate	306.1	344.1	-	352.5	348.7	371.9	-
A1B_Land use	333.0	356.3	380.7	-	-	386.3	346.2
B1_Land use	333.0	357.5	380.7	-	362.7	386.3	351.1
A1B_Climate+Land use	306.3	335.5	360.2	-	-	363.3	324.9
B1_Climate+Land use	306.1	344.2	367.9	-	348.7	371.9	337.4

1099

1100

1101

1102

1103

1104

1105

1106

1107

1108

1109

1110

1111

1112

1113

1114 **Table 8.** Average sediment yield (tons ha⁻¹ y⁻¹) for the São Lourenço crops, under different climate
 1115 and land use scenarios. VINE – Vineyards; MPIN – Maritime pine; POTA – Potato; WPAS – Pasture;
 1116 PAST – Permanent pasture; EUCP – Eucalypt; MIXF – Mixed forests.

Scenarios	Sediment yield (tons ha ⁻¹ y ⁻¹)							
	VINE	MPIN	CORN	POTA	WPAS	PAST	EUCP	MIXF
Baseline	1.108	0.005	0.056	1.420	0.935	0.461	0.001	0.002
A1B_Climate	0.955	0.003	0.045	1.957	0.756	0.368	0.001	0.004
B1_Climate	0.962	0.003	0.044	1.778	1.074	0.500	0.001	0.004
A1B_Land use	1.108	0.005	0.051	-	-	-	0.002	-
B1_Land use	1.108	0.005	0.053	-	-	-	0.001	-
A1B_Climate+Land	0.952	0.004	0.041	-	-	-	0.002	-
B1_Climate+Land use	0.962	0.004	0.041	-	-	-	0.001	-

1117

1118

1119

1120

1121

1122

1123

1124

1125

1126

1127

1128

1129

1130

1131 **Table 9.** Average sediment yield (tons ha⁻¹ y⁻¹) for the Guadalupe crops, under different climate and
 1132 land use scenarios. FRSS – Cork/holm oak; SHRM – Mediterranean shrublands; WCRL – Wheat;
 1133 WPAS – Pasture; OLVG – Olive groves; SUNF – Sunflower.

Scenarios	Sediment yield (tons ha ⁻¹ y ⁻¹)					
	FRSS	SHRM	WCRL	WPAS	OLVG	SUNF
Baseline	0.091	-	1.359	0.089	2.928	-
A1B_Climate	0.082	-	2.167	0.111	2.675	-
B1_Climate	0.077	-	2.058	0.132	2.497	-
A1B_Land use	0.091	0.037	-	-	2.928	1.442
B1_Land use	0.091	0.037	-	0.087	2.928	1.672
A1B_Climate+Land use	0.082	0.032	-	-	2.675	1.297
B1_Climate+Land use	0.077	0.028	-	0.132	2.497	1.473

1134

1135

1136

1137

1138

1139

1140

1141

1142

1143

1144

1145

1146

1147

1148

1149
1150
1151
1152
1153
1154
1155
1156
1157
1158
1159
1160
1161
1162
1163
1164
1165
1166
1167
1168
1169
1170
1171
1172
1173

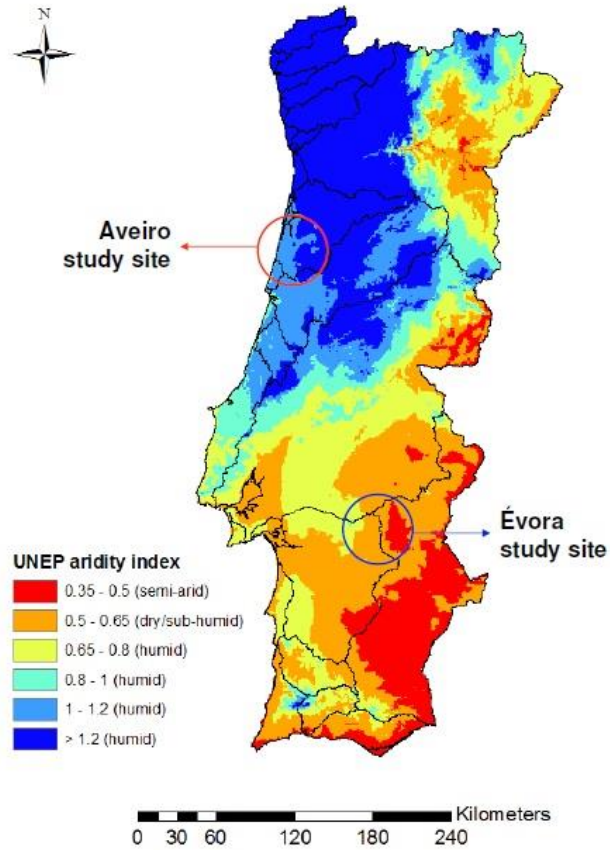


Fig. 1. Map of Portugal showing the location of the study sites and the UNEP aridity Index (Middleton and Thomas, 1997), calculated using spatial datasets for long-term average rainfall and potential evapotranspiration (SNIRH, 2014b).

1174
1175
1176
1177
1178
1179
1180
1181
1182
1183
1184
1185
1186
1187
1188
1189

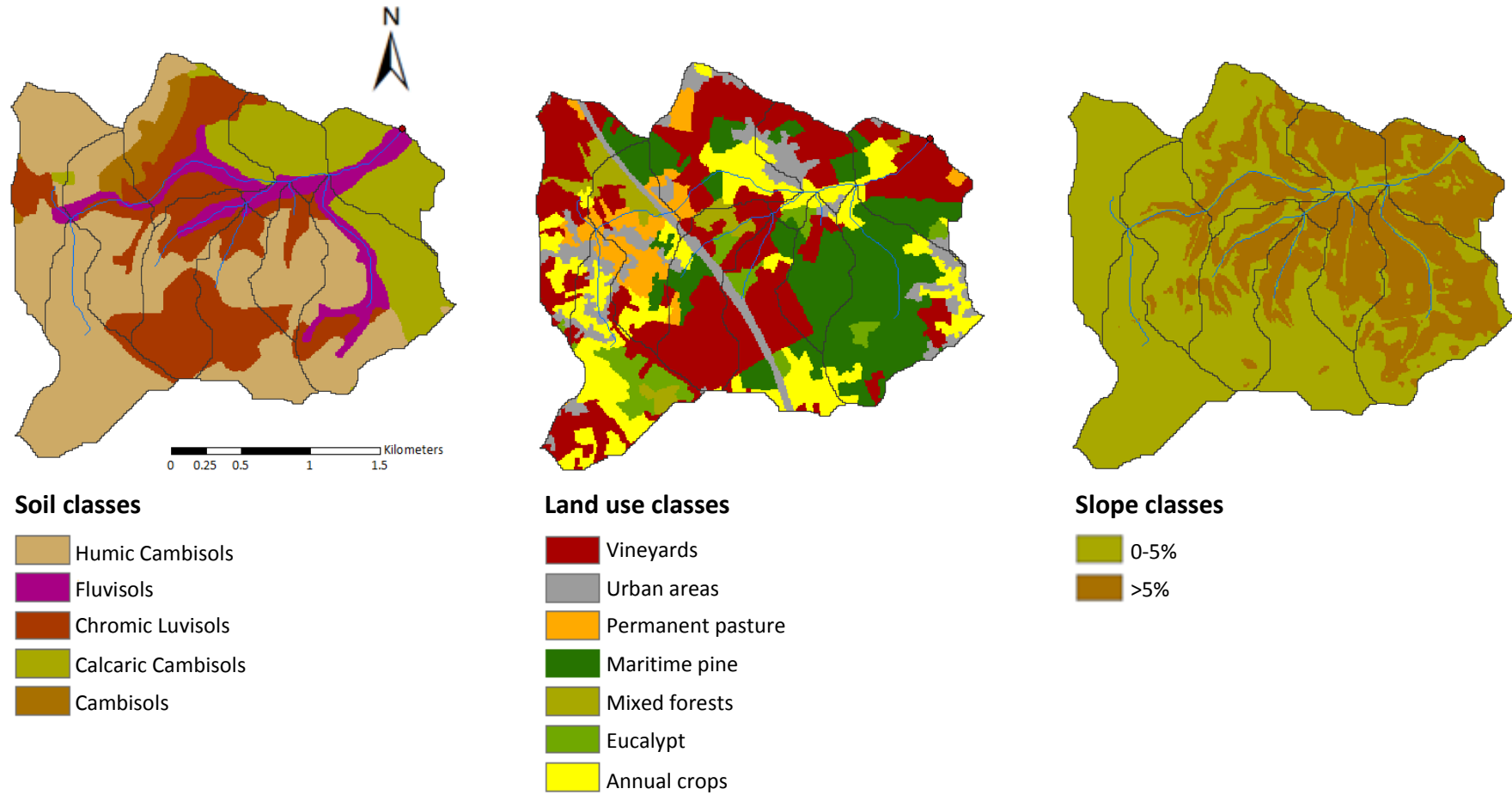
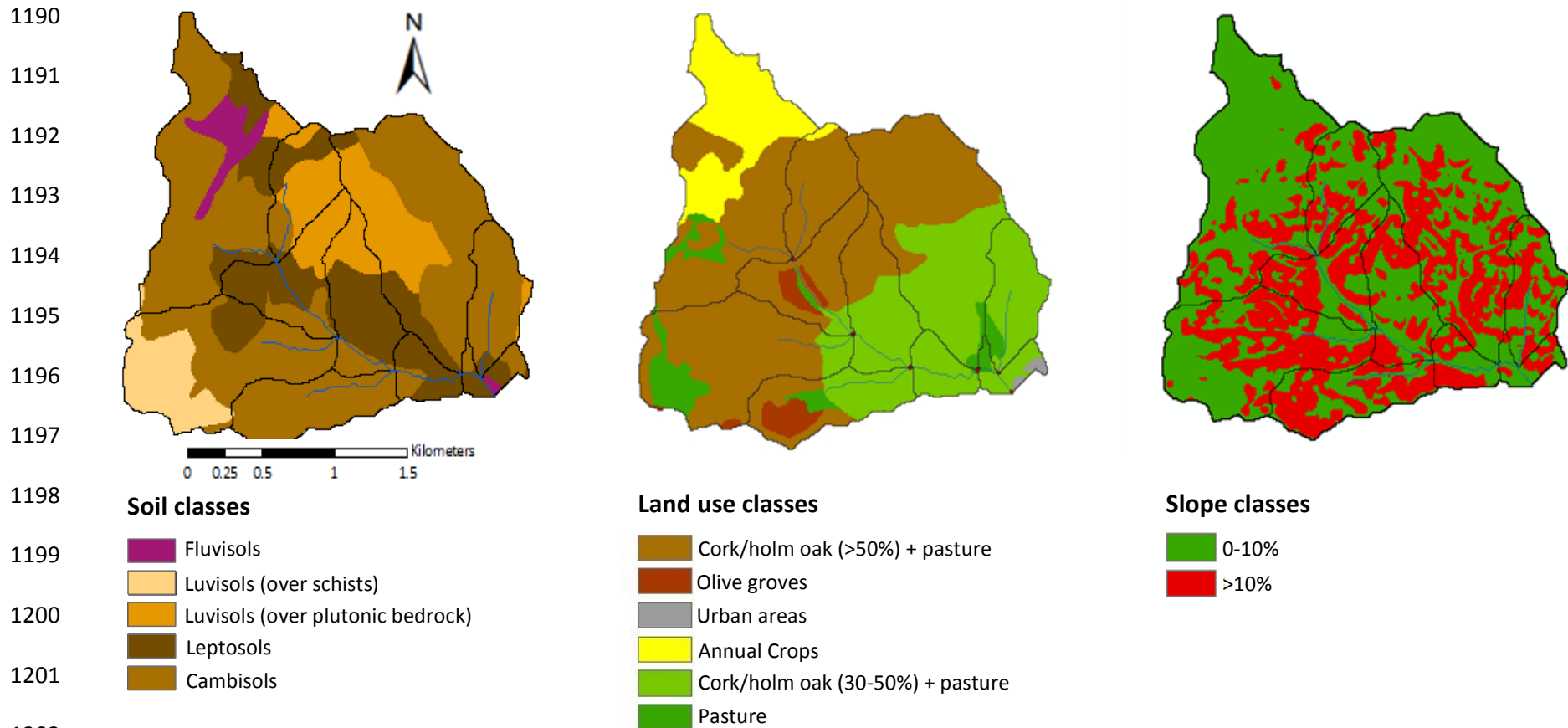


Fig. 2. Soil, land use and slope classes defined for São Lourenço.



1203 **Fig. 3.** Soil, land use and slope classes defined for Guadalupe.

1204

1205

1206
1207
1208
1209
1210
1211
1212
1213
1214
1215
1216
1217
1218
1219
1220
1221
1222
1223
1224
1225
1226
1227
1228
1229
1230
1231

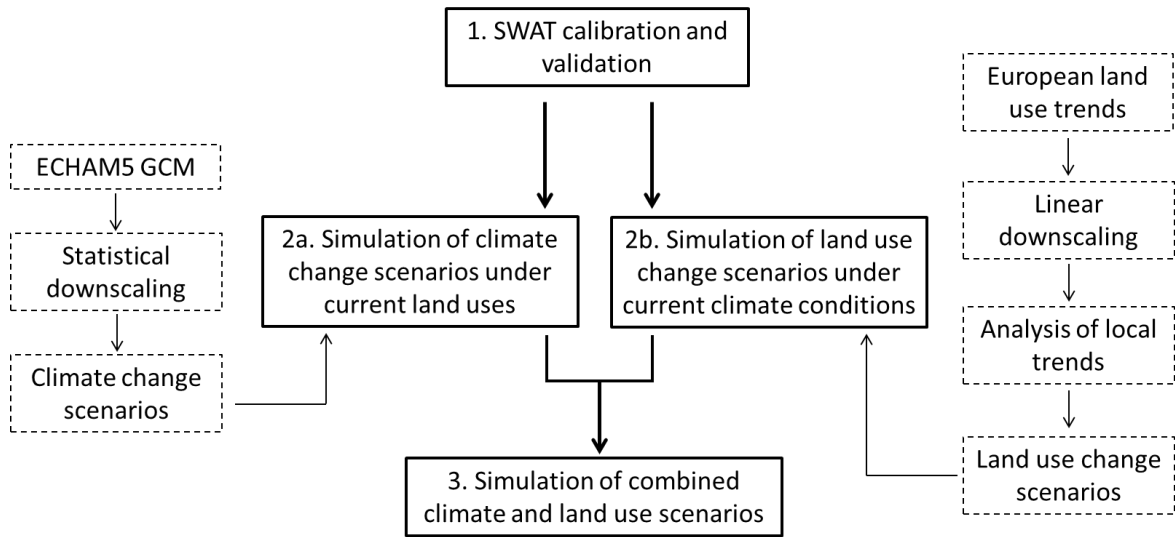


Fig. 4. Flowchart of the modelling work.

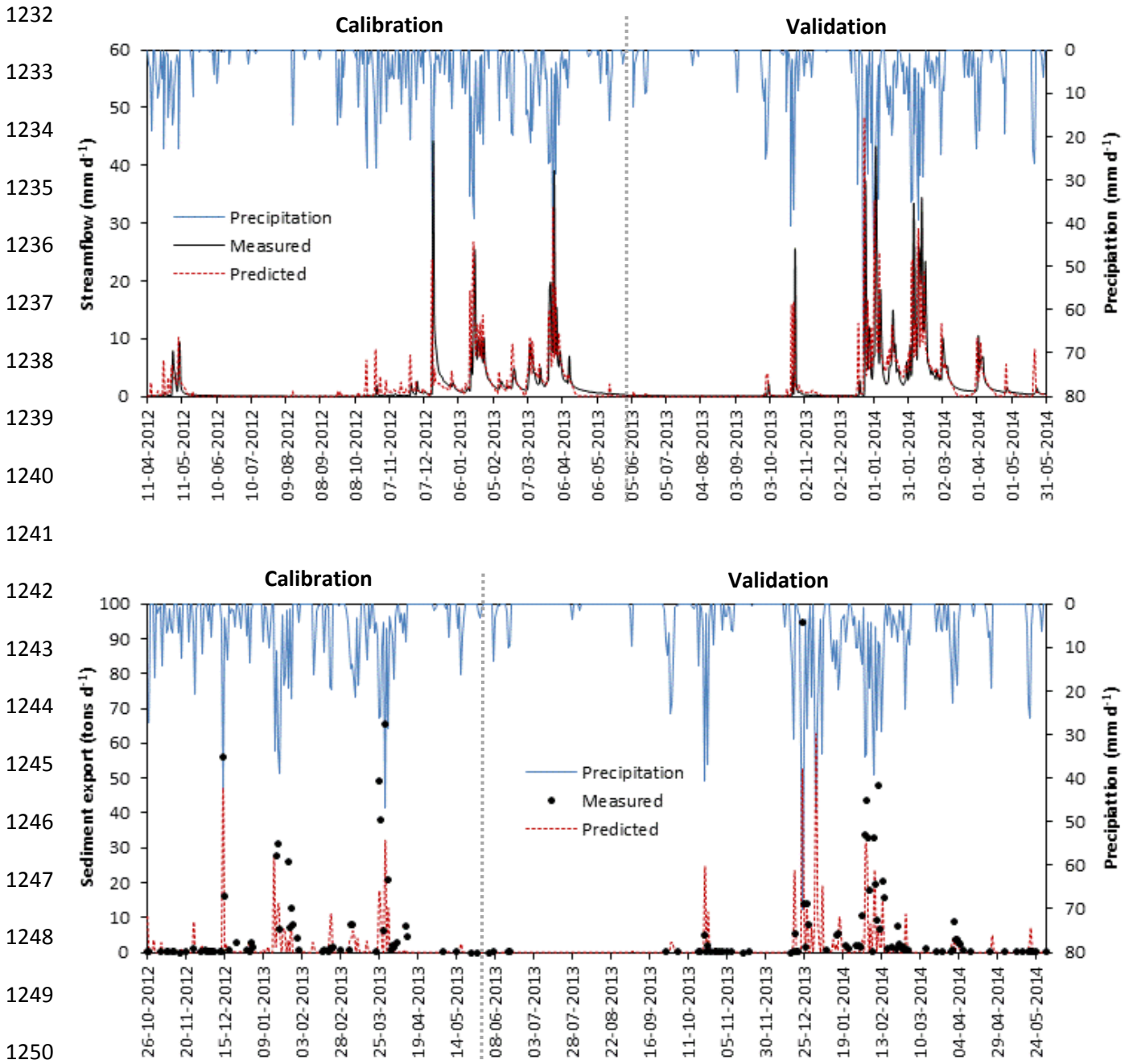
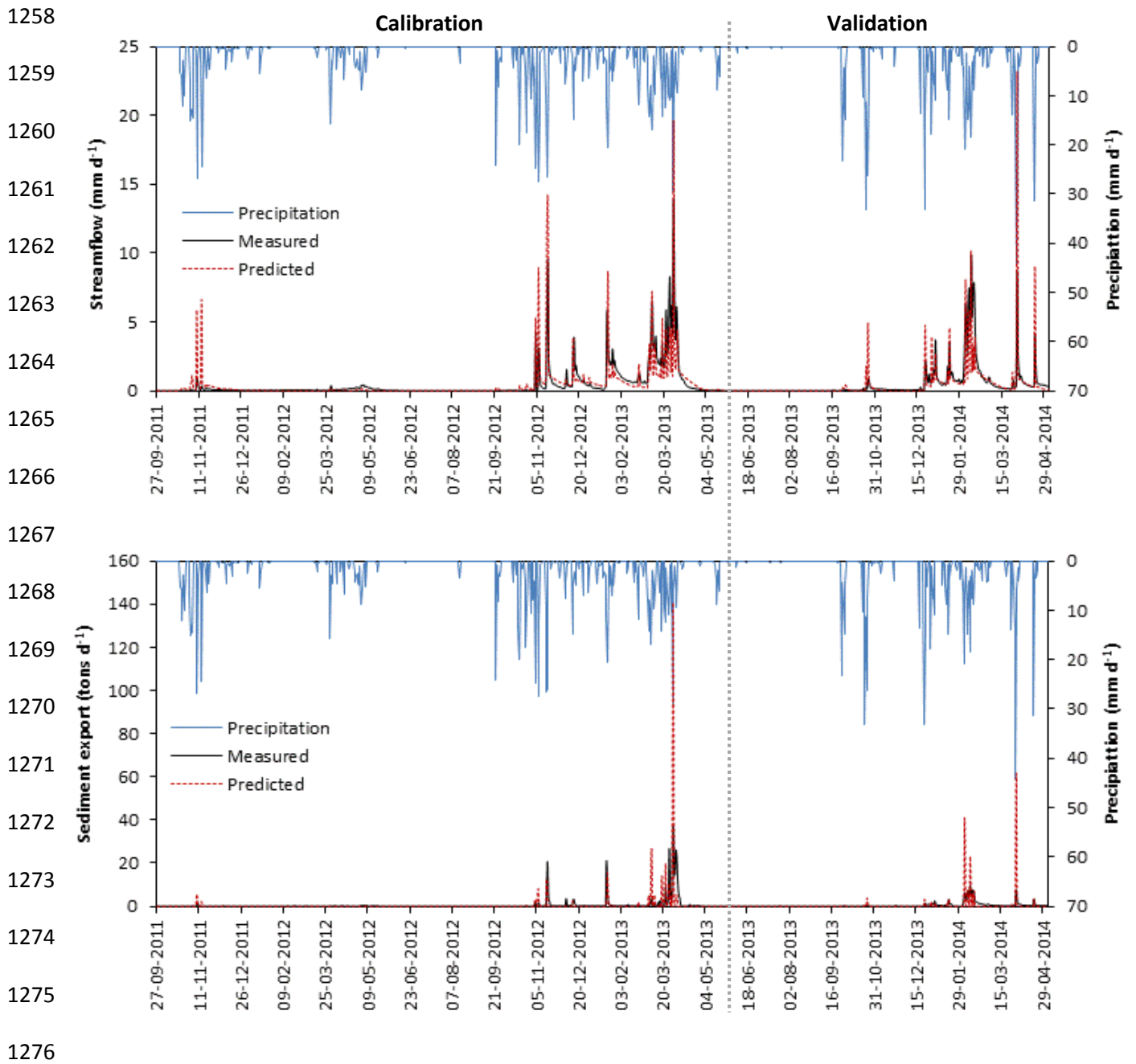


Fig. 5. Predicted and measured daily stream discharge (*top*) and sediment export (*bottom*) at the São Lourenço catchment, for the calibration and validation periods.



1277 **Fig. 6.** Predicted and measured monthly streamflow (*top*) and sediment export (*bottom*) at the
 1278 Guadalupe catchment, for the calibration and validation periods.

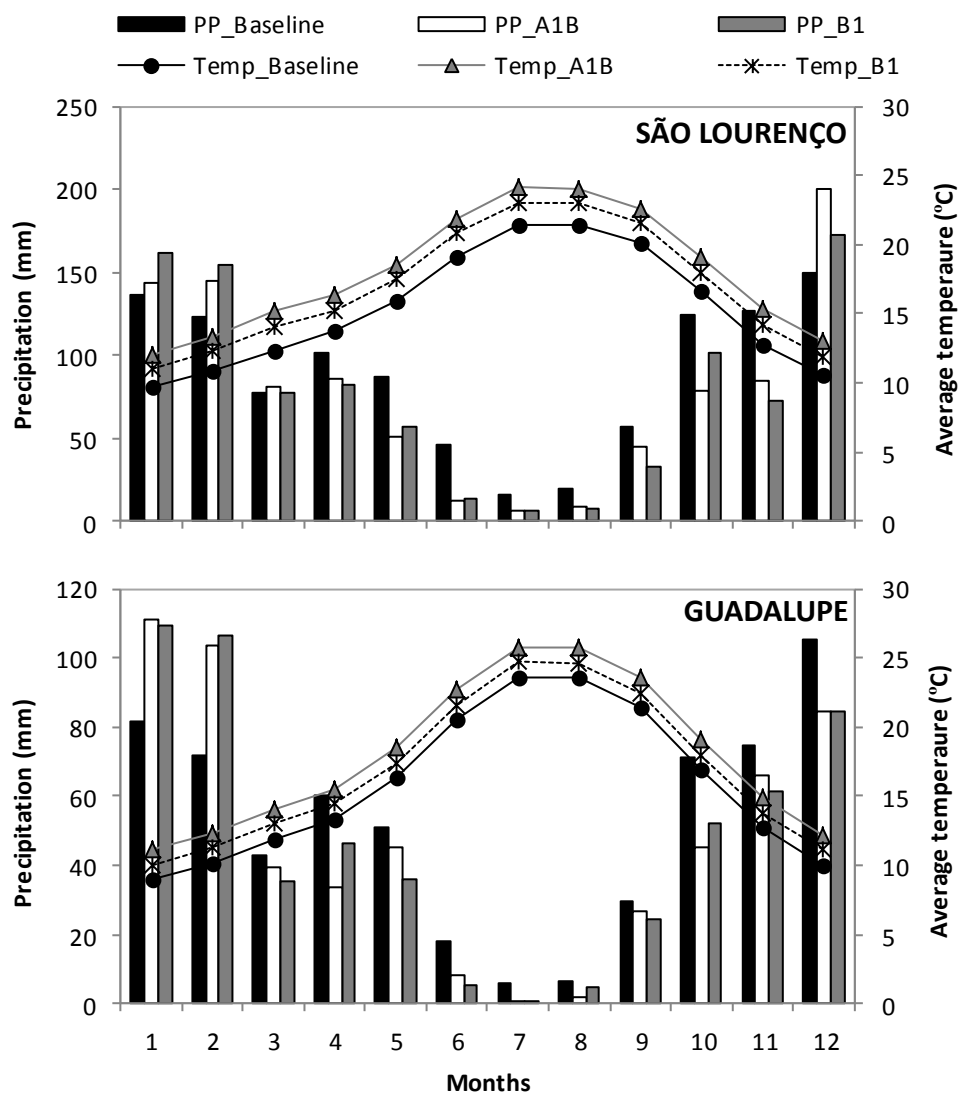
1279

1280

1281

1282

1283



1284

1285 **Fig. 7.** Average monthly temperature and precipitation for the baseline scenario (1971-2000) and
 1286 the A1B and B1 future emission scenarios (2071-2100), in the São Lourenço and Guadalupe
 1287 catchments.

1288

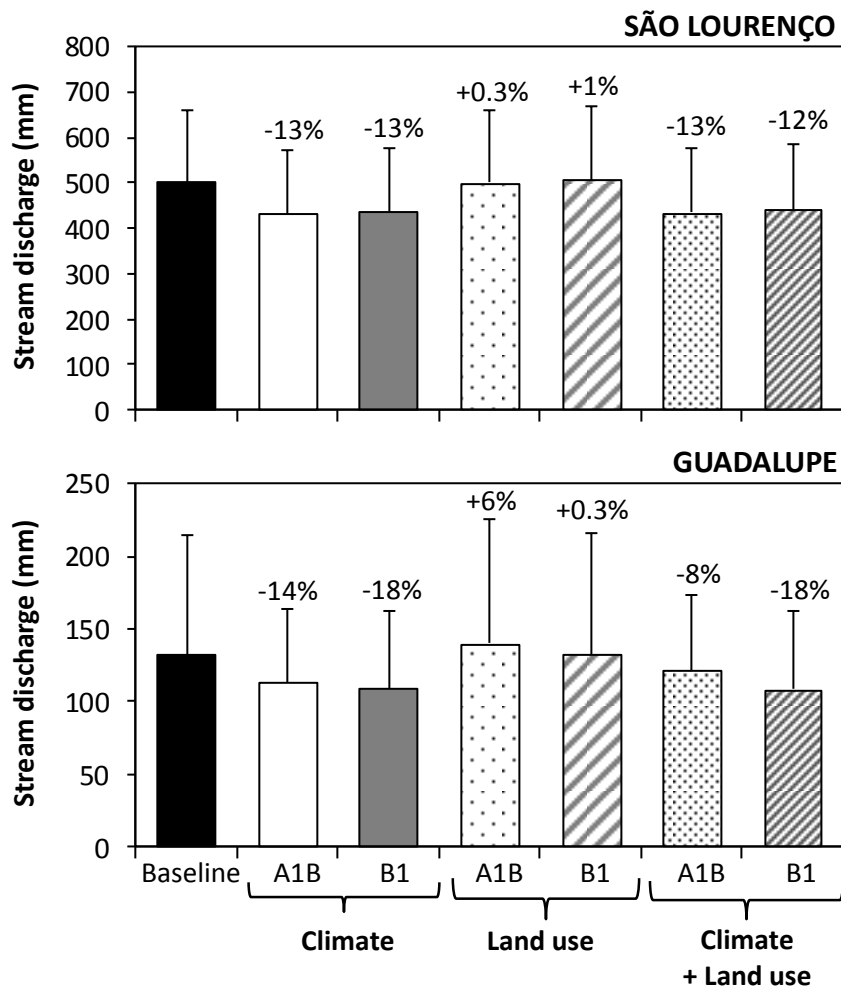
1289

1290

1291

1292

1293



1294

1295

1296 **Fig. 8.** Average annual (\pm standard deviation) stream discharge under different scenarios of

1297 climate, land use and combined climate and land use changes, in the São Lourenço and

1298 Guadalupe catchment.

1299

1300

1301

1302

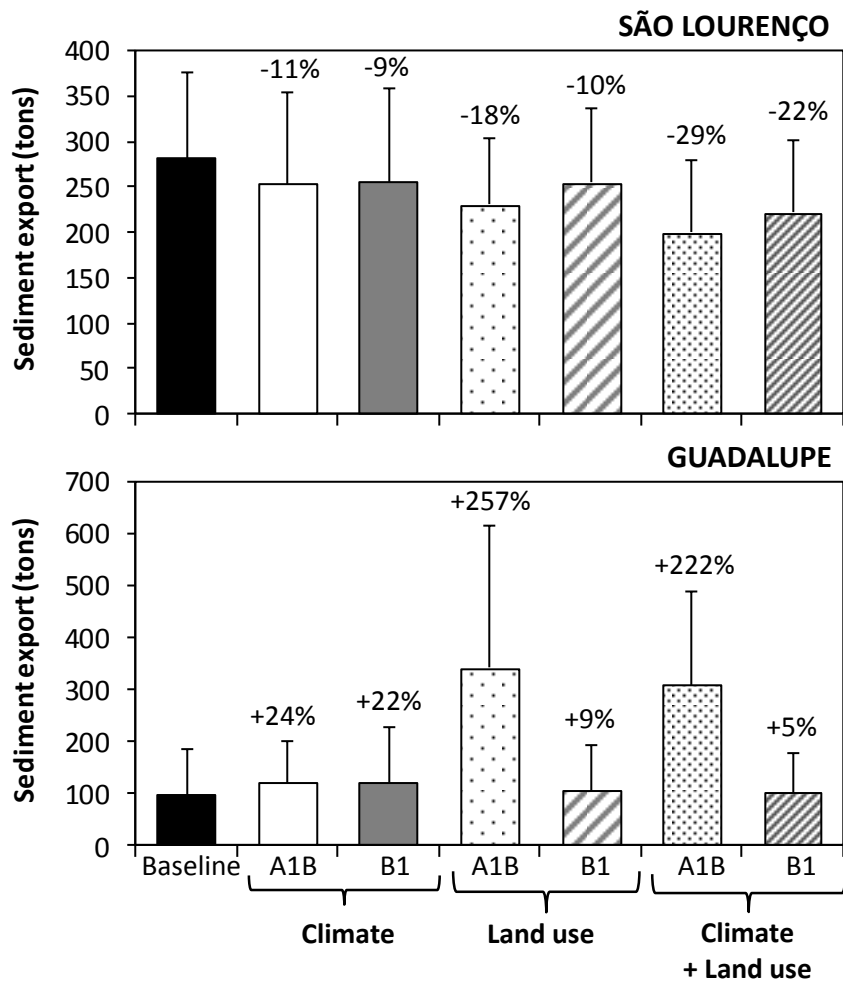
1303

1304

1305

1306

1307



1308

1309

1310 **Fig. 9.** Average annual (\pm standard deviation) sediment export under different scenarios of climate,

1311 land use and combined climate and land use changes, in the São Lourenço and Guadalupe

1312 catchment.

1313

1314

1315

1316

1317

1318

1319

1320

1321

1322

1323

1324

1325

1326

1327

1328

1329

1330

1331

1332

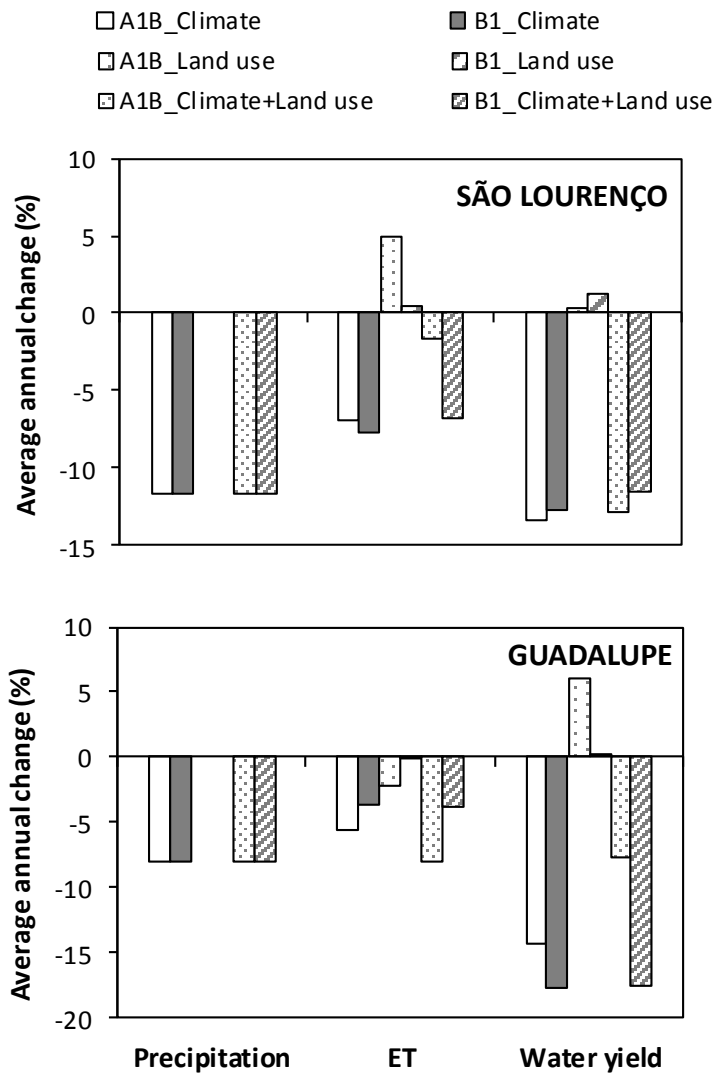
1333

1334

1335

1336

1337



1338 **Fig. 10.** Impacts of climate, land use and combined climate and land use change scenarios on the
 1339 water balance of the São Lourenço and Guadalupe catchments. ET – actual evapotranspiration.

1340